Review

Preclinical Testing Techniques: Paving the Way to New Oncology Screening Approaches

Antonia Van Rijt , Evan Stefanek , Karolina Valente *

Posted Date: 2 August 2023

doi: 10.20944/preprints202308.0109.v1

Keywords: preclinical; oncology; 3D culture; organ-on-a-chip; spheroid; organoid; 3D bioprinting; drug screening

Review

Preclinical Testing Techniques: Paving the Way to New Oncology Screening Approaches

Antonia van Rijt [1], Evan Stefanek [2] and Karolina Valente [1,*]

[1] Biomedical Engineering Program, University of Victoria, Victoria, BC V8P 5C2, Canada
[2] VoxCell BioInnovation Inc, Victoria, BC V8T 5L2, Canada; estefanek@voxcellbio.com
* Correspondence: kvalente@uvic.ca

Simple Summary: Traditional preclinical testing, including 2D cell culture and animal models, often fails to accurately predict drug efficacy in humans, especially for oncology drugs, where drug candidates that enter clinical trials have very high failure rates. Advancements in biology and tissue engineering techniques allow researchers to evaluate drug candidates before human trials using 3D cell culture models that more closely resemble human tissues than traditional methods. These techniques can better mimic the patterns of drug diffusion, cell-cell signaling, and the presence of vasculature in tumours *in vivo*. Furthermore, the FDA Modernization Act 2.0 promotes the use of higher complexity *in vitro* models such as 3D cell cultures. By offering more accurate representations of human tissue, 3D culture platforms have the potential to enhance preclinical drug development and lead to safer and more effective cancer treatments.

Abstract: Prior to clinical trials, preclinical testing of oncology drug candidates is performed by evaluating drug candidates with *in vitro* and *in vivo* platforms. For *in vivo* testing, animal models are used to evaluate the toxicity and efficacy of drug candidates. However, animal models often display poor translational results as many drugs that pass preclinical testing fail when tested in humans, with oncology drugs exhibiting especially poor acceptance rates. The FDA Modernization Act 2.0 promotes alternative preclinical testing techniques, presenting the opportunity to use higher complexity *in vitro* models as an alternative to *in vivo* testing, including 3D cell culture models. 3D tissue cultures address many of the shortcomings of 2D cultures by more closely replicating the tumour microenvironment through a combination of realistic drug diffusion, paracrine signaling, cellular phenotype, and vascularization that can better mimic native human tissue. This review will discuss the common forms of 3D cell culture, including cell spheroids, organoids, organs-on-a-chip, and 3D bioprinted tissues. Their advantages and limitations will be presented, aiming to discuss the use of these 3D models to accurately represent human tissue and as an alternative to animal testing. The use of 3D culture platforms for preclinical drug development is expected to accelerate as these platforms continue to improve in complexity, reliability, and translational predictivity.

Keywords: preclinical; oncology; 3D culture; organ-on-a-chip; spheroid; organoid; 3D bioprinting; drug screening

1. Introduction

Preclinical testing is a cornerstone of the drug development process and is responsible for preliminary studies of numerous compounds with the ultimate goal to lead to a safe and effective drug. The drug development process outlined by the FDA includes a series of stages to gain approval for market placement [1]. During the preclinical stage, screening of multiple compounds is performed with *in vitro* and *in vivo* platforms, including animal testing. 2D cell cultures are widely used in the preclinical stage to study the efficacy of cancer drugs, where cells are methodically exposed to therapeutic compounds and their responses are quantified. By studying which concentrations of drugs are effective on various types of cells, the response of the same cell types *in vivo* can be estimated. Additionally, drugs with mechanisms that block specific signaling pathways can be subjected to cells, which can then be lysed and analyzed through biochemical or multi-omic approaches [2]. However, 2D cell cultures (cell monolayers) used in preclinical testing lack the diverse

 doi:10.20944/preprints202308.0109.v1

cell populations and structure of human tissue, including the extracellular matrix (ECM) and accessory solutes. In addition, 2D cultures deliver a constant concentration of drug over a uniform cell monolayer, which is uncharacteristic of the dynamics in which a drug will diffuse through a tissue or tumour [3].

Animal models are a prolific tool in drug research and regulation, and they play a significant role in the preclinical stage. Through their integration in the pharmaceutical development and approval processes, animal models are utilized for their ability to mimic the response of the human body to prospective drugs [4]. Despite this, 90% of prospective drugs that pass the preclinical research stage fail in clinical trials, representing a significant inefficiency in the drug development process [5]. In addition, animal model results are not translatable and there is less than 8% correlation between *in vivo* data and clinical trials results.[3] Paired with the high failure rate of prospective drugs during preclinical testing, this reveals a stark need for preclinical testing techniques that more closely mimic human responses. This is especially true for anti-cancer drug development, where new therapies in the clinic a failure rate of 95% [6].

Following the preclinical stage, clinical trials are performed in 3 phases of increasing patient volume; Phase 1 gauges the safety of the product, Phase 2 investigates its effectiveness, and Phase 3 studies the overall drug performance on a larger and more diverse patient population. If the drug passes clinical testing, it proceeds to the new drug application (NDA) review stage, and approved drugs are monitored once they are on the market in the post-marketing stage [7]. The drug development timeline is a time- and resource-consuming task, with the entire process to lead to a single drug costing an excess of $1 billion over an average of 12 years [8].

In 2022, The United States Congress passed the FDA Modernization Act 2.0 to authorize alternative preclinical testing techniques as an exemption from animal testing [9]. In conjunction with recent developments in *in vitro* techniques, this could yield more promising clinical testing outcomes by increasing the accuracy of preclinical models. 3D *in vitro* cell culture models offer significant benefits over 2D cell cultures in their mimicry of human physiology and phenotypic features; however, the benefits of many 3D models need to be further validated before they can be widely adopted into the preclinical testing [10]. A variety of 3D *in vitro* methods can be used to validate drugs, including cell spheroids and organoids, organs-on-a-chip (OoCs), and 3D bioprinting techniques.

Cell spheroids are 3D aggregates of cells that better mimic the concentration gradient of a drug through a tissue when compared to 2D cultures [11]. Similar to spheroids, organoids are 3D structures of cells; however, they self-assemble using a hydrogel scaffold to form an extracellular environment and can have a variety of cell types with differentiated functions, allowing the organoid to have physiological properties closer to the intended organ [12]. While the lack of inherent vasculature in spheroids and organoids can allow the modeling of hypoxia and necrotic core of avascular tumours, these models fail to mimic truly vascularized tumors [13,14]. In addition, the lack of vasculature also inhibits nutrients from reaching the core of the structure, which can result in poor cell viability as their size increases and an inability to properly model drug delivery systems. Furthermore, the nutrient and oxygen gradients can influence cell growth, migration, and morphology [15].

Organs-on-a-chip (OoCs) are miniaturized microfluidic chips containing microscale tissues that more closely mimic the natural tissue behaviour [16,17]. OoCs are advantageous in replicating the mechanical processes of organs during typical physiological conditions and can model cellular interfaces between different organ compartments [18,19]. They can also be extended to multi-organ models to study interactions between tissues from different organs, providing more systemic insight during the drug development process [20]. However, while OoCs have superior tissue mimicry compared to 2D cultures, the complexity of *in vivo* tissues is still much greater [21].

3D bioprinting employs a variety of additive technologies combined with bioinks to produce 3D cellular structures [22]. Bioinks can be cell-laden or acellular, creating a scaffold for cells. 3D bioprinting allows for fine tuning of the model's 3D structure and a variety of bioinks can be used to closely replicate the mechanical structure of native human tissue, mimicking the ECM [23–25]. Common methods for 3D bioprinting include extrusion printing, digital light processing (DLP) printing, and 2-photon polymerization (2PP). During extrusion printing, bioink is extruded through a nozzle and deposited layer-by-layer on a build plate to create a 3D structure [26]. DLP printing uses light to selectively crosslink bioink from a liquid vat to produce layers of the 3D structure [27]. 2PP

 doi:10.20944/preprints202308.0109.v1

utilizes the energy from the absorption of two photons using a femtosecond laser to precisely crosslink material in the focal point of the laser in 3-dimensional space, or the voxel [28]. The resolution limitations of 3D bioprinting makes it difficult to print vascularized structures to study the uptake of drugs through the circulatory system; while the average capillary diameter is 5 μm, bioprinting using hydrogels can yield resolutions of 100 μm through extrusion printing, 25 μm using DLP, and 100 nm using 2PP [29–34].

The advantages and limitations of *in vitro* preclinical testing platforms will be discussed with the ultimate goal of highlighting the most promising techniques for wider adoption with the support of the FDA Modernization Act 2.0.

2. Spheroids

2.1. Limitations of 2D Cell Culture

2D cell cultures are the most widely used method for toxicological screening and determining drug candidate efficacy during preclinical testing. 2D cell culture consists of either using primary cells or immortalized cell lines and growing them in an artificial environment. Primary cells are derived from living tissue which are then cultured *in vitro* and eventually become senescent, while immortalized cell lines can be cultured indefinitely. Primary cells may be more physiologically relevant due to phenotypic variation of patient tissues; however, immortalized cell lines provide a consistent genetic profile and are easy to obtain [35]. Typically, cells must be attached to a solid substrate, but certain cultures can be grown in a suspension of the culture medium. Cultures that are anchored to a solid substrate form a monolayer culture where the substrate surface, such as a petri dish, becomes covered by a single cell-thick layer of cells as they attach and proliferate [3,36]. 2D cell cultures are easy to grow and proliferate quickly, so they present a convenient way to gather preliminary data on drug toxicity [37]. However, 2D cultures do not fully depict human tissue due to the lack of 3D properties, so they may not predict clinical physiological responses to compounds with accuracy. In addition, in 2D cultures, constant concentration of the drug is deposited across the entire cell monolayer, whereas *in vivo* tissues will induce a concentration gradient from where the drug is delivered. Furthermore, native human tissue has additional constituents that exist alongside cells to regulate structure and function, such as the ECM, which gives mechanical structure to the tissue while also supplementing growth factors and other bioactive molecules to regulate cell characteristics [38]. 2D cultures also limit paracrine cellular interactions since signaling between adjacent cells is limited to 2 dimensions. Cell phenotype can also be altered when cultured in 2D, which can be partially mitigated by co-culturing in 2D with multiple cell types [39]. However, tumour tissue is composed of cancer cells along with healthy stromal cells, such as endothelial cells, stem cells, and fibroblasts which biochemically support the tumour microenvironment and are involved in paracrine signaling [40,41]. 2D co-cultures still cannot fully recreate the tumour microenvironment due to their limited contact with adjacent cells and lack of tumour-stroma interactions.

2.2. Spheroids for Preclinical Drug Development

Cell spheroids were created to increase the predictivity of cell monolayers, taking preclinical testing to a further degree of complexity. Cell spheroids are 3D aggregates of cells typically formed by seeding cells onto a non-adherent substrate or hanging drop, allowing the cells to assemble into a 3D structure rather than forming a 2D monolayer. Various methods for establishing spheroid culture are visually depicted in Figure 1. Spheroids are especially useful at modeling cancers, which have complex invasive behaviours, feedback mechanisms, and tumour-stromal cell interactions [42]. Spheroids form due to cell-cell adhesion from their integrin proteins and ECM proteins. Cells initially aggregate due to the binding of cell-surface integrin and leads to the upregulation of cadherin expression. This causes an accumulation of cadherin on the cell membrane, and the resulting cadherin-cadherin binding between cells strengthens the connections of adjacent cells to form the spheroid [43]. Integrins also play a role in the activation of focal adhesion kinase (FAK), a tyrosine kinase that participates in cell adhesion, migration, and growth. FAK influences cellular structure through the actin filaments in the cytoskeleton, which is integral for spheroid formation. In relation to cancer modeling, FAK overexpression is also associated with invasive tumour phenotypes, so spheroids help give a more faithful representation of tumour behaviour [44]. Spheroids also boast greater longevity than 2D cultures since they can be cultured for up to four weeks, whereas 2D

Preprints (www.preprints.org) | NOT PEER-REVIEWED | Posted: 2 August 2023 doi:10.20944/preprints202308.0109.v1

cultures typically reach confluency within a week. Spheroids could thus be a better candidate for lasting studies to determine long-term effects of drugs on surviving cells [37]. A summary of methods for formulating spheroids with their respective advantages and limitations can be found in Table 1. In total, spheroids most closely capture tissue behaviour when they possess three key characteristics: a constitution of different cell types capable of cell-cell interactions, an ECM for mechanical stability and regulating cell function, and nutrient media with the required nutrients for tissue differentiation and maturation [42]. A summary of methods for establishing spheroid cultures can be found in Table 1.

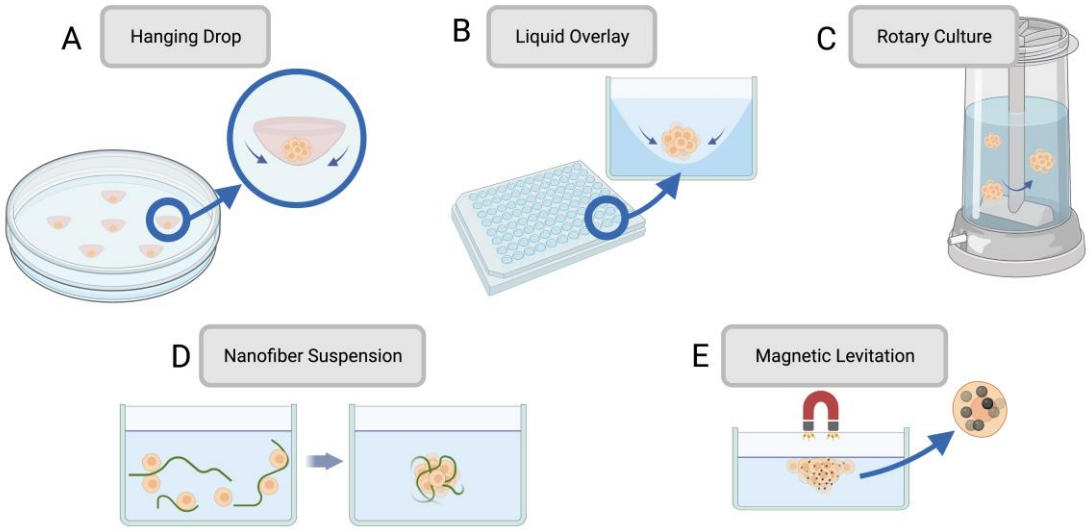

Figure 1. Common methods for producing spheroids for preclinical drug development such as (A) hanging drop, (B) liquid overlay, (C) rotary culture, (D) nanofiber suspension, and € magnetic levitation. Created with BioRender.com.

Table 1. Technical overviews of spheroid fabrication methods with respective advantages and disadvantages.

Spheroid Fabrication Method	Overview	Advantages	Drawbacks	References
Hanging drop	A drop of cell suspension is placed onto the inside of a cell culture plate lid, which is then inverted without disturbing the droplets held by surface tension. Over time, cells concentrate and cluster into a spheroid at the bottom of the hanging droplet.	• Simple • Requires no specialized equipment • Can be used with small cell suspension volumes	• Laborious • Low throughput • High shear force • Limited cell lines form spheroids through this method	[45,46]
Liquid Overlay	Cell suspension is seeded onto a nonadherent surface with recesses that promote cell aggregation.	• High throughput • Control over spheroid size	• Some cell lines may need added ECM proteins to promote spheroid formation	[47,48]
Rotary cell culture	Cells are cultured in a container with an agitator that disrupts the cells' ability to adhere to the substrate, forcing them to self-assemble into spheroids.	• Simple • High throughput • Large scale	• Spheroid size variation • Viability challenges due to mechanical damage	[43,49,50]

Preprints (www.preprints.org) | NOT PEER-REVIEWED | Posted: 2 August 2023 doi:10.20944/preprints202308.0109.v1

Nanofiber cell suspension	Adding polymer nanofibers to the cell suspension increases spheroid production by cells interacting with the nanofibers.	• Reduced cell death due to non-adherence • Suitable for anchorage-dependent cells • More time-efficient than other adaptations for anchorage-dependent cells	• Polymer nanofibers may have unintended impacts on cell behaviour	[51–53]
Magnetic levitation	Magnetic particles are combined with cells, and a magnetic force is introduced. Negative magnetophoresis induces a weightless environment where cell aggregation is promoted	• Low-cost • Allows for real-time imaging • Minimizes additional forces on cells	• Can lead to apoptosis	[54–56]

2.3. Spheroids for Drug Efficacy

Cell spheroids' mimicry of the tumour microenvironment and metastatic tumour behaviour can be harnessed in diverse ways to study anticancer drugs. Cancer spheroids have been used to study the effects of anticancer drug cisplatin on different cancer types [57]. The spheroids were formed using 96-well spheroid microplates and centrifugation, and different cell types including HeLa, A459, 293T, SH-SY5Y, and U-2OS. These spheroids were exposed to cisplatin and ATP generation was monitored in real-time for 7 days, allowing for more long-term testing than is available for 2D cultures, which become contact inhibited once confluent, resulting in behavioural changes from cell cycle arrest. In particular, the tumour-stroma interactions of the tumour microenvironment have been modeled using spheroids across various cancer types. Pancreatic stellate cells, a stromal cell type, have been cultured using spheroids with pancreatic cancer cells to investigate how the microenvironment influences the progression of pancreatic ductal adenocarcinoma. The co-cultured model exhibited resistance to gemcitabine and heightened migration when compared to the cancer cells cultured alone, emulating chemo-resistant, invasive, and metastatic phenotypes [58]. Spheroids have also been used to model metastatic pathways between different tissues for high-throughput drug testing. Co-culture spheroid hydrogels were previously used to produce a heterotypic model for prostate-to-bone cancer metastasis [59]. Despite breakthroughs in therapeutics, prostate cancer remains the second most frequently diagnosed cancer and the sixth leading cause of cancer death globally for men [60], and prognosis worsens for metastatic incidences of prostate cancer, which typically presents itself as metastasis through the bone. Models for prostate-to-bone cancer metastasis were made by spotting in-air 3D droplets of prostate cancer cells co-cultured with osteoblasts onto a superhydrophobic surface. The spheroidal 3D microgels were composed of methacrylated hyaluronic acid (HA-MA) and methacrylated gelatin (GelMA). The co-cultured cells and physiological conditions were replicated by using PC-3 cells initiated from a bone metastasis of a stage IV prostatic adenocarcinoma and human osteoblasts, which then exhibited mineralization through calcium deposits on the spheroid surface. The heterotypic 3D microgels demonstrated higher resistance to platin chemotherapeutics than comparable single or co-culture spheroids without the heterotypic prostate-bone interface [59].

2.4. Spheroids for Drug Toxicity

Previously, NIH3T3 fibroblasts were used as stromal cells in hanging-drop spheroid co-culture with ovarian adenocarcinoma cells and pancreatic epithelioid carcinoma cells, respectively. The fibroblasts were engineered with a reporter gene whose signal could be monitored over time in media to determine the cytotoxic effects on the stromal cells compared to the cancer cells. This helped to identify a therapeutic window and provides opportunities to distinguish between broadly cytotoxic compounds and those that target cancer cells more selectively [61]. Co-cultured tumour spheroids have been used to study the efficacy of blocking cell membrane receptors NKG2A and MICA/B in therapies for colorectal cancer (CRC) [62]. NKG2A and NKG2D are receptors on natural killer (NK) immune cells, where NKG2A inhibits and NKG2D activates NK function. These NK receptors have

 doi:10.20944/preprints202308.0109.v1

promising therapeutic potential for cancers such as CRC that are resistant to immunomodulation. Cellular infiltration of NK cells was enhanced by targeting NKG2D and its ligands MICA and MICB, resulting in more efficient destruction of CRC spheroids and demonstrating their potential for anticancer therapies.

3. Organoids

Like spheroids, organoids are 3D cell culture structures grown *in vitro*. However, organoids and spheroids have some key differences that give them strengths and limitations for various applications. Cell spheroids are aggregated together through weak forces such as proteins interactions and adhesion molecules, and while they can be co-cultured to better recapitulate tumour phenotype, they are relatively simple and do not possess the diverse differentiation of living tissues. Organoids, on the other hand, are more complex structures with differentiation and organization to mimic the function as well as the structure of a given organ [63,64]. Furthermore, while spheroids can be formed with discrete cell types, some types of organoids can differentiate into distinct populations of functional cells. However, while organoids offer greater complexity and functionally replicate target organs, they are more difficult to produce than spheroids, since spheroids can be generated easily and in large quantities due to their simplicity [65].

Organoids are prime candidates for investigations regarding specific aspects of organ function, while spheroids are better suited for high-throughput testing. Due to their advantages in modeling specific functions of human tissue, organoids have been harnessed to study intricate mechanisms of cancer, such as patient-specific drug resistance, genomics, and phenotype.

Organoids for Preclinical Drug Development

Organoids derived from primary cancer cells are beneficial for studying variation in how cancers are presented across different patients and offer significant future possibilities for personalized medicine. In a previous study, organoids were derived from human lung, kidney, and gastric cancer cells from patients and cultured in Matrigel using a pair of synchronized modules to deliver droplets into a 96-well plate [66]. The first module, M1, is a microfluidic mixer that manipulates the Matrigel and cools it to workable low temperatures. M1 forms droplets by combining the Matrigel and cell solution with an immiscible oil, which form cell laden Matrigel droplets in the cooled environment. The droplets are then heated in the same segment of tubing to transition to a gelled state. The second module, M2, then automatically dispenses the 3D organoid droplets in a 96-well plate. Using this automated system, the droplets developed into organotypic constructs larger than 400 μm within 5-7 days rather than the 4-6 weeks traditionally required for growing organoids of this size and were highly reproducible. The organoids conserved 97% of gene mutations from the primary tumour and were 80% accurate in recapitulating drug sensitivity variations between patients. As such, this automated organoid model shows promise for personalized medicine through rapid drug screening for cancer patients. Preclinical opportunities for organoids in cancer screening was also seen in a previous ovarian cancer (OC) model where tumour samples from epithelial OC patients were dissociated and cultured as organoids [67]. The organoids themselves recapitulated original tumour phenotypes, which was determined through immunohistological and immunofluorescence analyses targeting gene markers and mutation of the tumour-suppressor protein p53, which is characteristic of the high-grade serous OCs investigated in this model. Furthermore, through DNA sequencing, the organoids reproduced the genetic structure of the primary tumours. Most importantly, the organoids exhibited sensitivities to clinical chemotherapy drugs that were congruent with individual patient responses. In conjunction, this OC model establishes that organoids can closely recapitulate primary tumour genomics and phenotype and can realistically model patient-specific chemotherapy responses when compared to clinical data. A cancer-screening organoid model was also studied for human gastric cancer [68]. In this model, organoids were sourced from gastric cancer patients with resected gastric cancer tumours and were subjected to standard-of-care chemotherapy. Organoids that showed resistance to the chemotherapeutics were sourced from patients with poor chemotherapy responses, indicating that the organoids were suitable at predicting patient drug sensitivities. Furthermore, RNA sequencing confirmed that the organoids closely resembled the primary tumour tissue.

 doi:10.20944/preprints202308.0109.v1

4. Organ-On-A-Chip

OoCs are microscale systems that consolidate advancements in tissue engineering and microfluidic chips to mimic specific physiological tissue environments. Microfluidic chips use microscale channels that are configured in specific ways to manipulate small volumes of fluid, from picolitres to milliliters [69,70]. By integrating hydrogels mimicking miniature tissue models inside microfluidic chips, OoCs can circulate blood or nutrients to the tissue with a high degree of control. Using leading microfabrication technologies, OoCs can maintain highly controlled cell microenvironments and more closely recapitulate tumour phenotypes than 2D cell models [71]. Due to the decreased reagent consumption and increasingly simple fabrication methods associated with microfluidic technology, OoCs can reduce overall costs in preclinical testing while also better predicting physiological responses [72].

4.1. Single-organ and Multi-Organ Chips

Single-organ models can be used to study the specific organ responses to a particular compound; additionally, the adaptable nature of microfluidic chips allows for multiple organ compartments to be integrated in one multi-organ system for monitoring interactions between different tissues in phenomena such as cancer metastasis or paracrine signaling [73]. Tissue models used in OoCs can include lab-grown organoids or primary samples obtained from patients. Lab-grown organoids are easier to grow in large quantities and have a relatively consistent genotypic profile, so they can be beneficial in high-throughput drug screening. However, while they are complex structures, lab-grown organoids may not reflect the complete heterogeneity of human tumours, which can affect their responses to drugs. This is due to the importance of supporting cell types, immune cells, and the stroma in the tumour microenvironment. Furthermore, stromal cells and immune cells utilize signaling pathways to influence inflammation and tumour progression as well as ECM deposition [74,75] Conversely, benefits of primary samples include that they retain the characteristics of the patient's tumour, which allows for personalized medicine opportunities and reflects inter-patient differences in drug response between patients with the same type of cancer [76]. However, primary samples are difficult to obtain in high quantities and have greater variation, making it difficult to interpret test results for high-throughput testing. In total, cell source selection is dependent on the goals and purpose of the project.

4.2. OoC Architecture

Device architecture is another point of consideration in OoC design. Typically, OoCs can be categorized into two main construction styles that denote their general function and purpose. The first type, solid organ chips, are comprised of 3D tissue masses that are positioned in the microfluidic chip such that they can interact with one another and the culture medium in specific ways. Solid organ chips can be used to model parenchymal or mesenchymal tissues for studying general tissue responses and properties [77]. The second type, barrier tissue chips, has a structure that allows the formation of a cellular barrier separating discrete fluid paths. This models the function of living barriers between endothelial and epithelial tissues and allows for the study of molecule transport or different responses between compartments [78]. Photolithography has long been used for the precise microfabrication of silicon, which offers opportunities for integration of electronic components in OoCs; however, it is brittle and has poor optical properties [79]. Other commonly used materials for the fabrication of OoCs include polydimethylsiloxane (PDMS), glass, 3D printing resins, and thermoplastics such as polymethylmethacrylate (PMMA) and cyclic olefin copolymer (COC), each with their own benefits and drawbacks. PDMS offers high resolution and has a relatively inexpensive and simple fabrication process using soft lithography but is susceptible to absorbing and subsequently leaching various chemicals which can be detrimental to experiment reproducibility [80,81]. Glass OoCs are inert but are significantly more expensive to produce and have extensive manufacturing processes [82]. 3D printing resins offers benefits for iterative testing due to their rapid prototyping but have poor optical properties and little supporting literature for resin biocompatibility [83,84]. Thermoplastics are suitable for injection molding in mass-produced OoC systems, but can have sealing difficulties since typical bonding techniques used in soft lithography do not translate well to PMMA chips [85–87]. As there are many benefits and drawbacks surrounding OoC fabrication, each design should be assessed to determine the most suitable method.

Preprints (www.preprints.org) | NOT PEER-REVIEWED | Posted: 2 August 2023 doi:10.20944/preprints202308.0109.v1

Table 2. Comparison of common materials for OoC including their suitable fabrication methods and the advantages and drawbacks for each.

Material	Fabrication method	Advantages	Drawbacks	References
Polydimethylsiloxane (PDMS)	Soft Lithography	• Optically clear • Recapitulates high detail • Easy fabrication • Permeable to gasses • Hydrophilic/ hydrophobic capabilities • Biocompatible	• Absorption, retention, and release of small molecules • Laborious for mass production	[80,81]
Polymethylmethacrylate (PMMA)	Injection Molding	• Optically clear • Minimal absorption • Cost-effective for mass production	• High stiffness • Low fidelity in complex microstructures • Low gas permeability • Difficult to seal	[86,87]
Cyclic olefin copolymer (COC)	Injection Molding	• Optically clear • Minimal absorption • Cost-effective for mass production	• High stiffness • Low fidelity in complex microstructures • Low gas permeability • Difficult to seal	[85]
Silicon	Photolithography	• Compatible with electronic integration • Versatile surface treatments • Recapitulates high detail	• Laborious and costly to produce • Requires cleanroom facilities • Poor optical transparency • Brittle	[79]
Glass	Etching	• Optically clear • Inert • Chemically resistant • Biocompatible	• Laborious and costly to produce • Brittle	[82]
Resins	3D Printing	• Low cost • Rapid prototyping • High throughput	• Poor optical properties • Poor biocompatibility • Low permeability • Texturally rough • Low fidelity in complex microstructures	[83,84]

4.3. OoC for Preclinical Drug Development

OoCs hold promise for cancer drug screening by offering physiological relevance while retaining experimental controllability and reproducibility [17]. Cardiotoxicity is a cause of concern for anti-cancer drugs since cardiac safety is not always recapitulated in current preclinical animal models. The human ether-a-go-go-related gene (hERG) encodes a subunit of a potassium channel and plays a significant role in cardiac repolarization. Blocking hERG leads to long QT syndrome and associated fatal arrhythmias The blockage of hERG is the most common cause of cardiotoxicity, and as a result, evaluating the effect of drugs on hERG can indicate prospective cardiotoxicity levels [88]. An integrated OoC was previously created to evaluate anti-tumour drug efficacy and cardiac safety for listinib as a treatment for Ewing Sarcoma (ES), which demonstrated promise for treating ES in preclinical xenograft models but had a high incidence of patients with relapsed or refractory ES in clinical testing [89]. The polysulfone-based OoC with cultured bone ES tumour tissues for recreating the ES microenvironment and heart muscle tissues was circulated with listinib and its response to the drug was compared to clinical results. Results from this integrated setting exhibited minimized

 doi:10.20944/preprints202308.0109.v1

tumour reduction and less cardiotoxicity than the xenograft models that predicted significant decreases in tumour and cardiac function. In total, the OoC system had more congruent results with clinical trial data than the current xenograft model and has opportunities to be extended to other drug and tissue systems. OoC can also be harnessed to mimic vascularized structures due to their ability to finely manipulate very small quantities of fluid. OoC have previously been used to produce vascularized micro-organs and micro-tissues for studying the effects of anticancer drugs using self-assembled vascularized tissues [90]. In this study, a device was fabricated using a PDMS microfluidic layer with three connected chambers and a transparent polymer membrane bonded to a bottomless 96-well plate, and self-assembled vascularization was achieved through the cell-laden gel matrix by subjecting the chambers to gravimetric flow for one week. Additionally, healthy vascularized micro-organs (VMOs) were fabricated using normal human lung fibroblasts and endothelial progenitor cell lines, with a colorectal cancer cell line added to the vascularized micro-tumours (VMTs). Vascular permeability was quantified using mathematical models, and the tissues were perfused with chemotherapy drugs fluorouracil, vincristine, and sorafenib to monitor their influence on the vasculature and surrounding structures. The microfluidic chip was able to successfully form self-assembled vascularized models and confirmed that vincristine is a vascular disrupter while fluorouracil is not. Furthermore, the platform boasted high reproducibility, indicating its potential use for high-throughput testing. A similar three-chamber OoC was used to create colorectal cancer VMTs where the structures better recapitulated gene expression and chemotherapy responses of parallel xenograft tests when compared with monocultures and 3D spheroids [91]. Additionally, the VMT vasculature exhibited leakiness that is associated with in-vivo tumours and better mimicked the heterogeneous tumour microenvironment by recreating tumour-stroma interactions that are correlated with native human tumours.

4.4. Vascularization Capabilities of OoCs

Vascularized OoC for phenotypic screening have also been fabricated using injection molding for high-throughput testing. A microfluidic system was previously designed using sequentially patterned hydrogels in a microfluidic body to induce the formation of perfusable vascular networks [92]. The platform setup, dubbed the MicroVascular Injection-Molded Plastic Array 3D Culture (MV-IMPACT), is an injection molded device, allowing it to be produced in high volumes with little variation. Assembly of vascular networks in a central section of fibrin gel seeded with endothelial cells was facilitated by lung fibroblasts in fibrin gel on each side, and human colorectal adenocarcinoma and hepatocellular carcinoma were incorporated to recapitulate heterogeneous tumour-stroma interactions of the tumour microenvironment. The MV-IMPACT was used to validate the efficacy of DAPT, a drug associated with the formation of thicker and more numerous angiogenic vessels through Notch signaling pathway inhibition. Groups treated with DAPT exhibited increased vessel thickness and branching, which was congruent with similar experiments using *in vivo* techniques. By utilizing injection molding and a compact design, the platform shows promise for high-throughput testing with decreased reagent consumption, increasing *in vitro* test efficiency and accessibility.

5. D Bioprinting

3D printing is an additive fabrication technique that utilizes sequentially produced layers that are combined to produce a final 3D structure [93]. Using thermoplastics, photosensitive resins, or metal, 3D printing can produce intricate rapid prototypes for iterative testing and can also be used in final manufacturing stages [94,95]. 3D bioprinting combines these principles with biological materials, cells, and supporting biomolecules to produce detailed tissue-like 3D structures that can closely mimic real tissue physiology. 3D bioprinting is beneficial for tissue modeling as it can be used to produce vascularized structures and their biochemical and mechanical properties can be finely tuned through bioink selection [96]. Overall biomimicry of tissue models is dependent on the specific method of 3D bioprinting and biomaterials used [97,98]. A summary of common 3D bioprinting methods can be found in Figure 2.

Preprints (www.preprints.org) | NOT PEER-REVIEWED | Posted: 2 August 2023 doi:10.20944/preprints202308.0109.v1

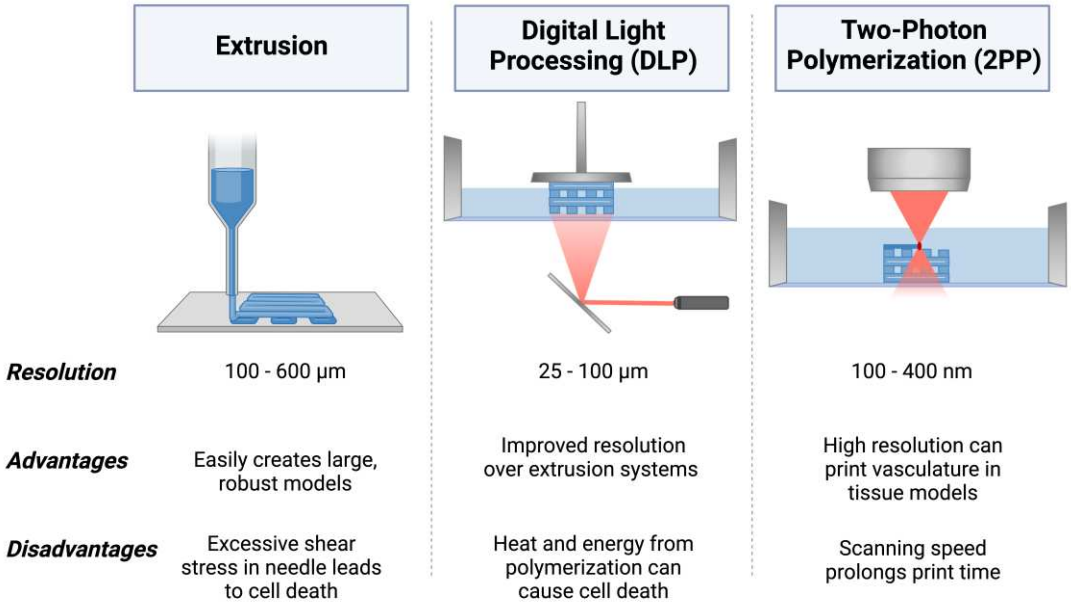

Figure 2. Schematic of common methods of 3D bioprinting including **(A)** extrusion, **(B)** digital light processing (DLP), and **(C)** two-photon polymerization (2PP). Created with BioRender.com.

5.1. Extrusion 3D Bioprinting

Extrusion bioprinting dispenses bioink through a nozzle onto a substrate using a series of motors for precise movement of the printhead and building stage. Upon being dispensed by the nozzle, the printed material may be either ionically crosslinked or photo-crosslinked [99,100]. Furthermore, multi-printhead systems can be used to produce structures with a variety of materials for more heterogeneous structures or for sacrificial supports. Bioinks with shear-thinning properties can be beneficial for extrusion bioprinting as the sharp convergence of the nozzle causes these materials to decrease in viscosity, allowing the bioink to flow through the nozzle more easily and become more structurally stable again from their increased viscosity after deposition. This can also improve cell viability since unregulated shear force at the nozzle can damage cells and lead to cell death [101,102]. Extrusion bioprinting can be performed with very high cell densities, which is important for accurately recreating native tissues [103]. Resolutions of 100-600 µm can be achieved through extrusion bioprinting and producing intricate structures such as vascular networks can be challenging [30,31].

5.2. Digital Light Processing (DLP) 3D Bioprinting

DLP is a type of light-based 3D bioprinting utilizes specific wavelengths of light to selectively polymerize liquid bioink in a reservoir. Polymerization is achieved through the activation of a photoinitiator in the bioink. DLP polymerizes an entire layer of bioink at a time using a digital micromirror device (DMD) projector [104,105]. As such, bioinks are restricted to light-activated materials. Resolutions of 25-100 µm can be achieved through DLP bioprinting, producing more complex structures such as vascular networks with some success, especially with synthetic polymers [104]. DNA damage from UV exposure and cytotoxic species formed through the photoactivation process can both be detrimental to cell health, but photoinitiators with improved biocompatibility that are active in the visible light spectra such as LAP have reduced the severity of this issue [106].

5.3. Two-Photon Polymerization (2PP) 3D Bioprinting

TPP 3D bioprinting is a direct writing method that utilizes a femtosecond laser to selectively polymerize bioink with a high degree of precision. TPP harnesses two-photon absorption theory, where the simultaneous absorption of two photons by a photosensitive molecule increases the energy state of the molecule, initiating the polymerization of the material at the focal point of the laser [32]. Since crosslinking only occurs at the voxel, light can pass through areas of the material without polymerizing it. The polymerization at the voxel can yield resolutions down to 100-400 nm, allowing

Preprints (www.preprints.org) | NOT PEER-REVIEWED | Posted: 2 August 2023 doi:10.20944/preprints202308.0109.v1

for bioprinting detailed structures with high precision, including more intricate vascular patterns [107]. While various photoinitiators exhibit promising biocompatibility, some may negatively impact cell viability through the potential to produce volatile species during their activation mechanism [108,109]. Furthermore, the wavelengths of light used in 2PP need to be considered to avoid cell damage due to irradiation at harmful wavelengths, such as UV light leading to apoptosis [110].

5.4. D Bioprinting Biomaterials

3D bioprinted structures are also characterized by their bioink constituents. Bioink components can be typically categorized into either natural or synthetic biomaterials, which have overarching traits that are common to each respective group. Natural biomaterials have complex biochemical traits and can closely mimic the ECM. This leads to favourable biocompatibility and cell adhesion, which allows cells to proliferate, differentiate, and migrate similarly to native tissues. However, due to inherent inconsistencies between sources of natural substances, naturally derived biomaterials often have significant variance between batches, making it difficult to produce bioinks with highly reproducible characteristics. Furthermore, they often have weak mechanical properties, so they may not be fit for mimicking more rigid tissues and are prone to degradation. Conversely, synthetic biomaterials have low variability and are highly reproducible, allowing for fine tuning of mechanical properties and degradation through the modification of functional groups of the polymer backbone. However, synthetic biomaterials do not mimic the ECM as closely as natural materials and may produce cytotoxic by-products upon degradation that can be detrimental to biocompatibility [111]. A variety of commonly used natural and synthetic biomaterials can be found in Table 3 and Table 4, respectively. As such, bioinks that utilize both natural and synthetic biomaterials simultaneously can reap the benefits of both types while minimizing their limitations.

Table 3. Summary of common natural biomaterials with properties and crosslinking mechanics for use in bioinks.

Material	Overview	Properties for Bioinks	Crosslinking Mechanics	References
Collagen	Triple helical protein for tissue scaffolding and tensile strength in tendon, cartilage, bone, and skin	• Biodegradable • Biocompatible • Contributes to printability • Bioactive properties	Covalent bonding of fibrils	[112–114]
Gelatin	Hydrogel from the hydrolysis of collagen, solid when cooled and can be used to synthesize gelatin methacryloyl (GelMA)	• Temperature-based gelation • Printable • Tunable mechanical properties	Gelation under cold temperatures	[115–118]
Gelatin Methacryloyl (GelMA)	Gelatin derivative with methacrylated functional groups, mechanically stable after photocrosslinking	• Selective crosslinking • Mimics the ECM • Cell-binding sites • Biocompatible • Tunable	Photocrosslinked under UV light exposure	[119,120]
Fibrin	High-viscosity, insoluble biopolymer that allows for paracrine signalling due to non-linear elasticity	• Biocompatible • Biodegradable • Regenerative • Nanofibrous structural properties • Imitates both hard and soft tissues	Cleaved by thrombin which induces polymerization	[121–123]
Hyaluronic Acid	Bioresorbable material found in mammalian ECM, maintains a hydrated environment	• High porosity allows for compound diffusion • Must be combined with other biomaterials for bioink synthesis as it	Enzyme-crosslinking, Schiff-base reaction, thiol-	[124–129]

Preprints (www.preprints.org) | NOT PEER-REVIEWED | Posted: 2 August 2023 doi:10.20944/preprints202308.0109.v1

		lacks mechanical stability and cell adhesion alone	modified HA crosslinking, Diels-Alder click crosslinking, ionic crosslinking, photo-crosslinking	
Chitosan	Polysaccharide derived from chitin deacetylation with solubility at low pH levels	• Nontoxic • Bio-adhesive • Suitable for soft tissues due to low mechanical strength	Chemical crosslinking with glutaraldehyde (amine groups), or citric acid (covalent)	[130–132]
Alginate	Polymer derived from brown algae, can form hydrogels that mimic the ECM and be crosslinked through its aldehyde groups	• Biocompatible • Low cost • Low bioactivity • Can degrade easily due to hydrolytic degradation	Ionically crosslinked with divalent cations	[133–136]
Decellularized ECM	Produced by removing cellular components from tissues by chemical or physical processes	• Can retain tissue-specific behaviours post-decellularization • May not require additional crosslinking	Glutaraldehyde, thermal gelation	[137–140]

Table 4. Summary of common synthetic biomaterials with relevant properties for bioink applications.

Material	Overview	Properties for Bioinks	References
Polylactic acid (PLA)	Semi-crystalline structure with high molecular weight, used in extrusion-based bioprinting	• Useful for dental models • Accurate surface properties • Can be brittle • Cell-compatible	[141–143]
Poly(lactic-co-glycolic acid) (PLGA)	Synthesized through co-polymerization of both glycolic acid and lactic acid	• Can perform controlled drug release • Properties can be tuned through glycolic to lactic ratio	[144–147]
Poly(ethylene glycol) diacrylate (PEGDA)	Long-chain photo-crosslinkable monomer that forms hydrogels	• Photo-crosslinkability allows for use in light-based printing • Hydrophilic for cell maintenance and encapsulation • Modular though tunable functional groups	[148–150]
Poly e-caprolactone (PCL)	Semi-crystalline thermoplastic with high thermal stability, long degradation rate	• Rubber-like flexibility in physiological conditions • High permeability • Useful for bone models due to degradation rate	[151–153]

Preprints (www.preprints.org) | NOT PEER-REVIEWED | Posted: 2 August 2023 doi:10.20944/preprints202308.0109.v1

Poly(propylene fumarate) (PPF)	Linear unsaturated polyester with fumaric acid backbone chains	• High viscosity • Light-responsive • Useful in degradable materials as its ester bonds can be hydrolyzed, allowing for excretable products	[154–156]

5.5. D Bioprinting for Preclinical Drug Development

Due to its high degree of spatial control, 3D bioprinting shows significant promise for producing physiologically relevant preclinical models for a variety of cancer subtypes. An overview of recent studies using 3D bioprinting to create preclinical models for different cancer types can be seen in Figure 3. Breast cancer is among the most prevalent cancer types worldwide and has an abnormally high risk of death after diagnosis for many more years compared to other cancer types [157]. As such, breast cancer is the most commonly researched cancer type among experimental papers [158]. Laser-based 3D bioprinting techniques have been previously used to produce breast cancer spheroids with high spatial control. The printing system used laser direct-write (LDW) for patterning microstructures with cell-laden biomaterials where alginate loaded with human MDA-MB-231 cells was selectively ejected into microbeads and crosslinked using calcium ions to produce core-shelled breast cancer structures [27]. This model was especially useful for modeling the hypoxic and necrotic nature of tumour cores with a high degree of reproducibility, as excessively small microbeads would have insufficient hypoxia it their core, but excessively large microbeads would have an overly necrotic core which may not be characteristic of *in vivo* conditions due to angiogenesis and tumour vascularization. As such, this model shows promise for utilizing 3D bioprinting methods in high-throughput testing with high accuracy and precision.

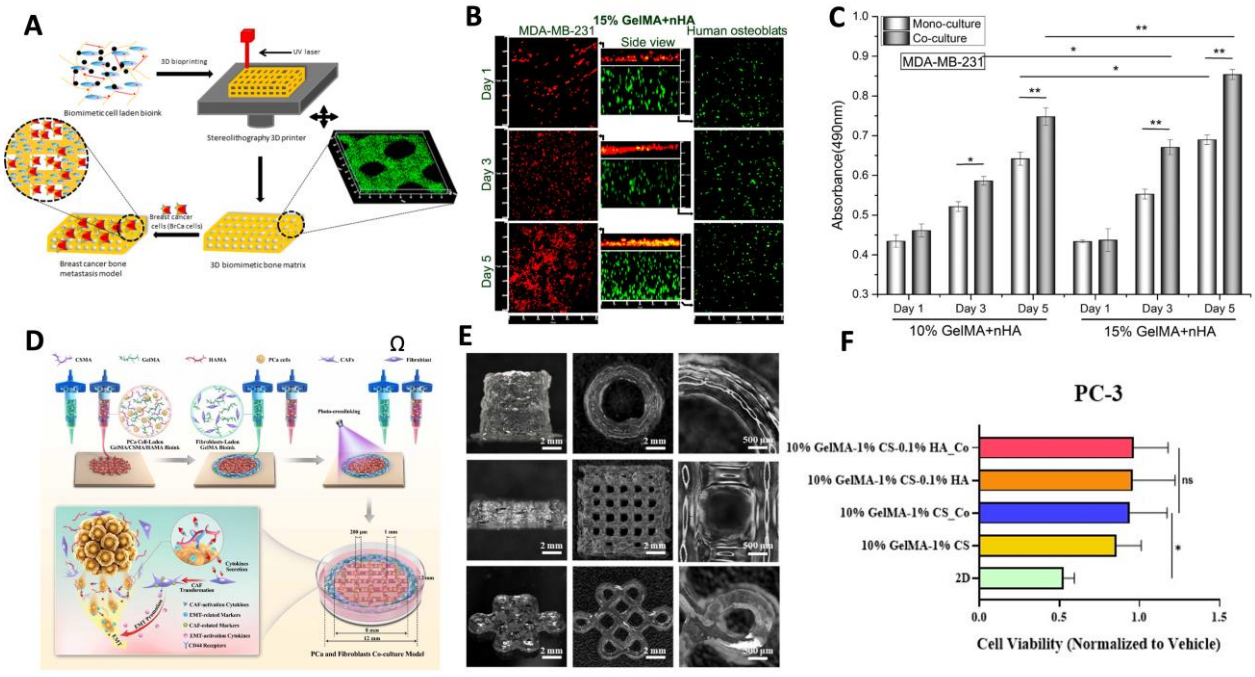

Figure 3. Recent 3D bioprinted cancer models for preclinical testing using **(A-C)** breast cancer and osteoblast co-culture [159] and **(D-F)** prostate cancer and fibroblast co-culture [160]. **(A)** Schematic diagram of light-activated 3D bioprinting process using cell-laden osteoblast scaffolding seeded with breast cancer cells to model breast cancer metastasis. **(B)** Confocal images of osteoblasts and breast cancer cells in co-culture after 1, 3, and 5 days. **(C)** Proliferation of breast cancer cells when cultured in mono-culture versus metastatic co-culture model with osteoblasts. **(D)** Schematic diagram of 3D bioprinting extrusion process for prostate and fibroblast co-culture model. **(E)** Extrusion printing of complex structures for prostate-fibroblast model. **(F)** DTX drug resistance of PC-3 (prostate cancer) cells in co-culture model. **(A-C)** Reprinted (adapted) with permission from [159]. Copyright 2016 American Chemical Society. **(D-E)** Reprinted under terms of the *Creative Commons Attribution 4.0 License* [160].

 doi:10.20944/preprints202308.0109.v1

5.6. D Bioprinting for Modeling Metastasis

Furthermore, tissues with diverse structural and mechanical properties can be fabricated using 3D bioprinting. The most common metastatic site for breast cancer is to the bone, and prognosis sharply worsens for patients once a metastatic state has been reached [161]. Traditional biomaterials can be used for modeling most soft tissues; however, a previous study incorporated nanocrystalline hydroxyapatite into GelMA bioink to study the interactive effects of cells in artificial bone microenvironments [159]. SLA printing was used to fabricate bone matrices laden with osteoblasts and bone marrow mesenchymal stem cells to which breast cancer cells were later introduced. Upon being introduced to the bone matrices, the breast cancer cells had enhanced growth and increased vascular endothelial growth factor. Conversely, the stromal bone cells had decreased proliferation and reduced alkaline phosphatase activity. In conjunction, these results indicate that 3D bioprinted co-cultures can help model the behaviours of complex metastatic cancer in post-metastatic stages.

5.7. Vascularization Capabilities of 3D Bioprinting

3D bioprinting is attractive due to its possibilities for vascularization strategies. Compared to other 3D cell culturing techniques, 3D bioprinting offers the most promise for producing specific and intentional vascular networks, especially with higher-resolution printing methods. This can be used to study various vascular phenomena of cancer, such as metastasis, angiogenesis, and oncologic drug uptake. A previous study utilized DLP techniques to fabricate honeycomb vascular-like structures with a variety of channel widths using PEGDA and studied the circulation of HeLa cervical cancer cells versus noncancerous 10 T1/2 cells [162]. While the noncancerous cells showed similar migration patterns regardless of channel width, the HeLa cells exhibited greater migration as channel width decreased. This trend is congruent with the cellular arrest and distant site proliferation characteristics of the metastatic process and suggests that 3D bioprinted vascular networks can be valuable tools in modeling metastatic cancers.

The vascular capabilities of 3D bioprinting can also be harnessed to produce 3D tissue cultures for diseases for which there are limited biomimetic models. Vascularized 3D bioprinted models have previously been studied for neuroblastoma (NB) by bioprinting multi-channel structures in HUVEC-lined GelMA and seeding NB spheroids at the core [163]. The vascularized outer structure was created by extruding GelMA into a support bath before being cured by UV, which were then seeded with HUVEC cells post-crosslinking. NB spheroids were cultured separately and were then manually added to the HUVEC-lined vascularized GelMA structures which were then dynamically cultured by rocking. The model exhibited an increase in NB aggressive behaviour through tumour cell migration and the integration of NB into the surrounding endothelial structures. Furthermore, by assessing the model's gene expression profile in post, the mechanisms for NB therapeutic responses can be studied.

6. Future Outlook

3D cell culture models mimic many aspects of the tumour microenvironment which allows them to provide preclinical insights on drug efficacy and toxicity that are not possible to obtain with 2D cultures. Although existing 3D culture models lack the complex interplay between organ systems that occurs in animals, these *in vitro* models could be a viable alternative for much of the preclinical testing performed in animals, including studies of target-tissue efficacy, liver toxicity, or kidney toxicity. Continuous development and validation of 3D culture models is required for these platforms to become adopted in the drug development process at larger scales. Validating the clinical relevance of results from 3D culture models with results from clinical trials is particularly important to demonstrate the advantages of 3D culture models. Although this can be performed retroactively, the strongest evidence on the benefits of 3D culture models or any new preclinical testing model is provided when the platform is used to guide the development of an active therapeutic and its clinical predictions are later confirmed in clinical trials. 3D culture models that are more standardized and thus relevant for use with drug candidates across a variety of indications will see quicker and wider adoption in the drug development process. Advantages of standardized 3D culture models are that they can be used across multiple pipelines within the same company, regulatory bodies are more likely to be familiar with interpreting their results, and much less time and resources are required to initially validate the model than with unique models.

Since animal models often fail to produce results that fully translate to clinical trials, 3D cultures also have a significant opportunity to provide better outcomes for patients by increasing the likelihood that innovative therapies succeed in clinical trials. Reducing the number of drug candidates that enter clinical trials to ultimately fail due to toxic side effects will also alleviate many of the adverse events that patients unfortunately experience in clinical trials. Discrepancies between animals and humans in metabolism, physiological differences, and disease states, all contribute to the lack of correlation between animal and clinical tests. Additionally, drug sensitivities and metabolic processes can differ between animal and human models which can cause disparities between how animal and human reactions to prospective drugs.

Author Contributions: Conceptualization, A.V.R. and K.V.; writing – original draft preparation, A.V.R.; writing – review and editing, E.S., K.V.; supervision, K.V. All authors have read and agreed to the published version of the manuscript.

Funding: This research received no external funding.

Institutional Review Board Statement: Not applicable.

Informed Consent Statement: Not applicable.

Data Availability Statement: Not applicable.

Conflicts of Interest: K.V. is the CEO of VoxCell BioInnovation Inc.

References

1. Bailey, A.M.; Mendicino, M.; Au, P. An FDA Perspective on Preclinical Development of Cell-Based Regenerative Medicine Products. *Nat Biotechnol* **2014**, *32*, 721–723, doi:10.1038/nbt.2971.
2. Yang, W.; Meng, L.; Chen, K.; Tian, C.; Peng, B.; Zhong, L.; Zhang, C.; Yang, X.; Zou, J.; Yang, S.; et al. Preclinical Pharmacodynamic Evaluation of a New Src/FOSL 1 Inhibitor, LY-1816, in Pancreatic Ductal Adenocarcinoma. *Cancer Sci* **2019**, *110*, 1408–1419, doi:10.1111/cas.13929.
3. Lovitt, C.; Shelper, T.; Avery, V. Advanced Cell Culture Techniques for Cancer Drug Discovery. *Biology (Basel)* **2014**, *3*, 345–367, doi:10.3390/biology3020345.
4. Ikeda, K.; Iwasaki, Y. Edaravone, a Free Radical Scavenger, Delayed Symptomatic and Pathological Progression of Motor Neuron Disease in the Wobbler Mouse. *PLoS One* **2015**, *10*, doi:10.1371/journal.pone.0140316.
5. Sun, D.; Gao, W.; Hu, H.; Zhou, S. Why 90% of Clinical Drug Development Fails and How to Improve It? *Acta Pharm Sin B* **2022**, *12*, 3049–3062, doi:10.1016/j.apsb.2022.02.002.
6. Unger, C.; Kramer, N.; Walzl, A.; Scherzer, M.; Hengstschläger, M.; Dolznig, H. Modeling Human Carcinomas: Physiologically Relevant 3D Models to Improve Anti-Cancer Drug Development. *Adv Drug Deliv Rev* 2014, *79*, 50–67.
7. Darrow, J.J.; Avorn, J.; Kesselheim, A.S. FDA Approval and Regulation of Pharmaceuticals, 1983-2018. *JAMA* **2020**, *323*, 164, doi:10.1001/jama.2019.20288.
8. van Norman, G.A. Drugs, Devices, and the FDA: Part 1: An Overview of Approval Processes for Drugs. *JACC Basic Transl Sci* **2016**, *1*, 170–179, doi:10.1016/j.jacbts.2016.03.002.
9. S.5002 - 117th Congress (2021-2022): FDA Modernization Act 2.0.
10. Andersen, T.; Auk-Emblem, P.; Dornish, M. 3D Cell Culture in Alginate Hydrogels. *Microarrays* **2015**, *4*, 133–161, doi:10.3390/microarrays4020133.
11. Gong, X.; Lin, C.; Cheng, J.; Su, J.; Zhao, H.; Liu, T.; Wen, X.; Zhao, P. Generation of Multicellular Tumor Spheroids with Microwell-Based Agarose Scaffolds for Drug Testing. *PLoS One* **2015**, *10*, e0130348, doi:10.1371/journal.pone.0130348.
12. Tuveson, D.; Clevers, H. Cancer Modeling Meets Human Organoid Technology. *Science (1979)* **2019**, *364*, 952–955, doi:10.1126/science.aaw6985.
13. Drasdo, D.; Höhme, S. A Single-Cell-Based Model of Tumor Growth in Vitro : Monolayers and Spheroids. *Phys Biol* **2005**, *2*, 133–147, doi:10.1088/1478-3975/2/3/001.
14. Barisam, M.; Saidi, M.; Kashaninejad, N.; Nguyen, N.-T. Prediction of Necrotic Core and Hypoxic Zone of Multicellular Spheroids in a Microbioreactor with a U-Shaped Barrier. *Micromachines (Basel)* **2018**, *9*, 94, doi:10.3390/mi9030094.
15. Glicklis, R.; Merchuk, J.C.; Cohen, S. Modeling Mass Transfer in Hepatocyte Spheroids via Cell Viability, Spheroid Size, and Hepatocellular Functions. *Biotechnol Bioeng* **2004**, *86*, 672–680, doi:10.1002/bit.20086.
16. Sun, W.; Luo, Z.; Lee, J.; Kim, H.-J.; Lee, K.; Tebon, P.; Feng, Y.; Dokmeci, M.R.; Sengupta, S.; Khademhosseini, A. Organ-on-a-Chip for Cancer and Immune Organs Modeling. *Adv Healthc Mater* **2019**, 1801363, doi:10.1002/adhm.201801363.

17. Ma, C.; Peng, Y.; Li, H.; Chen, W. Organ-on-a-Chip: A New Paradigm for Drug Development. *Trends Pharmacol Sci* 2021, *42*, 119–133.
18. Thompson, C.L.; Fu, S.; Heywood, H.K.; Knight, M.M.; Thorpe, S.D. Mechanical Stimulation: A Crucial Element of Organ-on-Chip Models. *Front Bioeng Biotechnol* **2020**, *8*, doi:10.3389/fbioe.2020.602646.
19. Kaarj; Yoon Methods of Delivering Mechanical Stimuli to Organ-on-a-Chip. *Micromachines (Basel)* **2019**, *10*, 700, doi:10.3390/mi10100700.
20. Satoh, T.; Sugiura, S.; Shin, K.; Onuki-Nagasaki, R.; Ishida, S.; Kikuchi, K.; Kakiki, M.; Kanamori, T. A Multi-Throughput Multi-Organ-on-a-Chip System on a Plate Formatted Pneumatic Pressure-Driven Medium Circulation Platform. *Lab Chip* **2018**, *18*, 115–125, doi:10.1039/C7LC00952F.
21. Danku, A.E.; Dulf, E.-H.; Braicu, C.; Jurj, A.; Berindan-Neagoe, I. Organ-On-A-Chip: A Survey of Technical Results and Problems. *Front Bioeng Biotechnol* **2022**, *10*, doi:10.3389/fbioe.2022.840674.
22. Datta, P.; Dey, M.; Ataie, Z.; Unutmaz, D.; Ozbolat, I.T. 3D Bioprinting for Reconstituting the Cancer Microenvironment. *NPJ Precis Oncol* **2020**, *4*, 18, doi:10.1038/s41698-020-0121-2.
23. Unagolla, J.M.; Jayasuriya, A.C. Hydrogel-Based 3D Bioprinting: A Comprehensive Review on Cell-Laden Hydrogels, Bioink Formulations, and Future Perspectives. *Appl Mater Today* **2020**, *18*, 100479, doi:10.1016/j.apmt.2019.100479.
24. Jia, L.; Zhang, Y.; Yao, L.; Zhang, P.; Ci, Z.; Zhang, W.; Miao, C.; Liang, X.; He, A.; Liu, Y.; et al. Regeneration of Human-Ear-Shaped Cartilage with Acellular Cartilage Matrix-Based Biomimetic Scaffolds. *Appl Mater Today* **2020**, *20*, 100639, doi:10.1016/j.apmt.2020.100639.
25. Elomaa, L.; Keshi, E.; Sauer, I.M.; Weinhart, M. Development of GelMA/PCL and DECM/PCL Resins for 3D Printing of Acellular in Vitro Tissue Scaffolds by Stereolithography. *Materials Science and Engineering: C* **2020**, *112*, 110958, doi:10.1016/j.msec.2020.110958.
26. Lewicki, J.; Bergman, J.; Kerins, C.; Hermanson, O. Optimization of 3D Bioprinting of Human Neuroblastoma Cells Using Sodium Alginate Hydrogel. *Bioprinting* **2019**, *16*, e00053, doi:10.1016/j.bprint.2019.e00053.
27. Kingsley, D.M.; Roberge, C.L.; Rudkouskaya, A.; Faulkner, D.E.; Barroso, M.; Intes, X.; Corr, D.T. Laser-Based 3D Bioprinting for Spatial and Size Control of Tumor Spheroids and Embryoid Bodies. *Acta Biomater* **2019**, *95*, 357–370, doi:10.1016/j.actbio.2019.02.014.
28. Hauptmann, N.; Lian, Q.; Ludolph, J.; Rothe, H.; Hildebrand, G.; Liefeith, K. Biomimetic Designer Scaffolds Made of D,L-Lactide-ε-Caprolactone Polymers by 2-Photon Polymerization. *Tissue Eng Part B Rev* **2019**, *25*, 167–186, doi:10.1089/ten.teb.2018.0284.
29. Potter, R.F.; Groom, A.C. Capillary Diameter and Geometry in Cardiac and Skeletal Muscle Studied by Means of Corrosion Casts. *Microvasc Res* **1983**, *25*, 68–84, doi:10.1016/0026-2862(83)90044-4.
30. Schwab, A.; Levato, R.; D'Este, M.; Piluso, S.; Eglin, D.; Malda, J. Printability and Shape Fidelity of Bioinks in 3D Bioprinting. *Chem Rev* **2020**, *120*, 11028–11055, doi:10.1021/acs.chemrev.0c00084.
31. Hinton, T.J.; Lee, A.; Feinberg, A.W. 3D Bioprinting from the Micrometer to Millimeter Length Scales: Size Does Matter. *Curr Opin Biomed Eng* **2017**, *1*, 31–37, doi:10.1016/j.cobme.2017.02.004.
32. Pawlicki, M.; Collins, H.A.; Denning, R.G.; Anderson, H.L. Two-Photon Absorption and the Design of Two-Photon Dyes. *Angewandte Chemie International Edition* **2009**, *48*, 3244–3266, doi:10.1002/anie.200805257.
33. Limberg, D.K.; Kang, J.-H.; Hayward, R.C. Triplet–Triplet Annihilation Photopolymerization for High-Resolution 3D Printing. *J Am Chem Soc* **2022**, *144*, 5226–5232, doi:10.1021/jacs.1c11022.
34. Valente, F.; Hepburn, M.S.; Chen, J.; Aldana, A.A.; Allardyce, B.J.; Shafei, S.; Doyle, B.J.; Kennedy, B.F.; Dilley, R.J. Bioprinting Silk Fibroin Using Two-Photon Lithography Enables Control over the Physico-Chemical Material Properties and Cellular Response. *Bioprinting* **2022**, *25*, e00183, doi:10.1016/j.bprint.2021.e00183.
35. Richter, M.; Piwocka, O.; Musielak, M.; Piotrowski, I.; Suchorska, W.M.; Trzeciak, T. From Donor to the Lab: A Fascinating Journey of Primary Cell Lines. *Front Cell Dev Biol* **2021**, *9*, doi:10.3389/fcell.2021.711381.
36. Saji Joseph, J.; Tebogo Malindisa, S.; Ntwasa, M. Two-Dimensional (2D) and Three-Dimensional (3D) Cell Culturing in Drug Discovery. In *Cell Culture*; IntechOpen, 2019.
37. Anton, D.; Burckel, H.; Josset, E.; Noel, G. Three-Dimensional Cell Culture: A Breakthrough in Vivo. *Int J Mol Sci* 2015, *16*, 5517–5527.
38. Yue, B. Biology of the Extracellular Matrix: An Overview. *J Glaucoma* 2014, *23*, S20–S23.
39. Kim, B.-S.; Nikolovski, J.; Bonadio, J.; Smiley, E.; Mooney, D.J. Engineered Smooth Muscle Tissues: Regulating Cell Phenotype with the Scaffold. *Exp Cell Res* **1999**, *251*, 318–328, doi:10.1006/excr.1999.4595.
40. 4Yin, Z.; Dong, C.; Jiang, K.; Xu, Z.; Li, R.; Guo, K.; Shao, S.; Wang, L. Heterogeneity of Cancer-Associated Fibroblasts and Roles in the Progression, Prognosis, and Therapy of Hepatocellular Carcinoma. *J Hematol Oncol* 2019, *12*.
41. Prager, B.C.; Xie, Q.; Bao, S.; Rich, J.N. Cancer Stem Cells: The Architects of the Tumor Ecosystem. *Cell Stem Cell* 2019, *24*, 41–53.
42. Jong, B.K. Three-Dimensional Tissue Culture Models in Cancer Biology. *Semin Cancer Biol* 2005, *15*, 365–377.

43. Białkowska, K.; Komorowski, P.; Bryszewska, M.; Miłowska, K. Spheroids as a Type of Three-Dimensional Cell Cultures—Examples of Methods of Preparation and the Most Important Application. *Int J Mol Sci* 2020, *21*, 1–17.
44. Tancioni, I.; Miller, N.L.G.; Uryu, S.; Lawson, C.; Jean, C.; Chen, X.L.; Kleinschmidt, E.G.; Schlaepfer, D.D. FAK Activity Protects Nucleostemin in Facilitating Breast Cancer Spheroid and Tumor Growth. *Breast Cancer Research* **2015**, *17*, doi:10.1186/s13058-015-0551-x.
45. Del Duca, D.; Werbowetski, T.; Del Maestro, R.F. Spheroid Preparation from Hanging Drops: Characterization of a Model of Brain Tumor Invasion. *J Neurooncol* **2004**, *67*, 295–303, doi:10.1023/B:NEON.0000024220.07063.70.
46. Foty, R. A Simple Hanging Drop Cell Culture Protocol for Generation of 3D Spheroids. *Journal of Visualized Experiments* **2011**, doi:10.3791/2720.
47. Mirab, F.; Kang, Y.J.; Majd, S. Preparation and Characterization of Size-Controlled Glioma Spheroids Using Agarose Hydrogel Microwells. *PLoS One* **2019**, *14*, e0211078, doi:10.1371/journal.pone.0211078.
48. Tang, Y.; Liu, J.; Chen, Y. Agarose Multi-Wells for Tumour Spheroid Formation and Anti-Cancer Drug Test. *Microelectron Eng* **2016**, *158*, 41–45, doi:10.1016/j.mee.2016.03.009.
49. Kang, S.; Kim, D.; Lee, J.; Takayama, S.; Park, J.Y. Engineered Microsystems for Spheroid and Organoid Studies. *Adv Healthc Mater* **2021**, *10*, 2001284, doi:10.1002/adhm.202001284.
50. Lin, R.-Z.; Chang, H.-Y. Recent Advances in Three-Dimensional Multicellular Spheroid Culture for Biomedical Research. *Biotechnol J* **2008**, *3*, 1172–1184, doi:10.1002/biot.200700228.
51. Kim, S.; Kim, E.M.; Yamamoto, M.; Park, H.; Shin, H. Engineering Multi-Cellular Spheroids for Tissue Engineering and Regenerative Medicine. *Adv Healthc Mater* **2020**, *9*, 2000608, doi:10.1002/adhm.202000608.
52. Ryu, J.H.; Kim, M.S.; Lee, G.M.; Choi, C.Y.; Kim, B.-S. The Enhancement of Recombinant Protein Production by Polymer Nanospheres in Cell Suspension Culture. *Biomaterials* **2005**, *26*, 2173–2181, doi:10.1016/j.biomaterials.2004.06.017.
53. Shin, J.-Y.; Park, J.; Jang, H.-K.; Lee, T.-J.; La, W.-G.; Bhang, S.H.; Kwon, I.K.; Kwon, O.H.; Kim, B.-S. Efficient Formation of Cell Spheroids Using Polymer Nanofibers. *Biotechnol Lett* **2012**, *34*, 795–803, doi:10.1007/s10529-011-0836-9.
54. Anil-Inevi, M.; Yaman, S.; Yildiz, A.A.; Mese, G.; Yalcin-Ozuysal, O.; Tekin, H.C.; Ozcivici, E. Biofabrication of in Situ Self Assembled 3D Cell Cultures in a Weightlessness Environment Generated Using Magnetic Levitation. *Sci Rep* **2018**, *8*, 7239, doi:10.1038/s41598-018-25718-9.
55. Souza, G.R.; Molina, J.R.; Raphael, R.M.; Ozawa, M.G.; Stark, D.J.; Levin, C.S.; Bronk, L.F.; Ananta, J.S.; Mandelin, J.; Georgescu, M.-M.; et al. Three-Dimensional Tissue Culture Based on Magnetic Cell Levitation. *Nat Nanotechnol* **2010**, *5*, 291–296, doi:10.1038/nnano.2010.23.
56. Türker, E.; Demirçak, N.; Arslan-Yildiz, A. Scaffold-Free Three-Dimensional Cell Culturing Using Magnetic Levitation. *Biomater Sci* **2018**, *6*, 1745–1753, doi:10.1039/C8BM00122G.
57. Baek, N.; Seo, O.W.; Lee, J.; Hulme, J.; An, S.S.A. Real-Time Monitoring of Cisplatin Cytotoxicity on Three-Dimensional Spheroid Tumor Cells. *Drug Des Devel Ther* **2016**, *10*, 2155–2165, doi:10.2147/DDDT.S108004.
58. Wong, C.W.; Han, H.W.; Tien, Y.W.; Hsu, S. hui Biomaterial Substrate-Derived Compact Cellular Spheroids Mimicking the Behavior of Pancreatic Cancer and Microenvironment. *Biomaterials* **2019**, *213*, doi:10.1016/j.biomaterials.2019.05.013.
59. Antunes, J.; Gaspar, V.M.; Ferreira, L.; Monteiro, M.; Henrique, R.; Jerónimo, C.; Mano, J.F. In-Air Production of 3D Co-Culture Tumor Spheroid Hydrogels for Expedited Drug Screening. *Acta Biomater* **2019**, *94*, 392–409, doi:10.1016/j.actbio.2019.06.012.
60. Culp, M.B.B.; Soerjomataram, I.; Efstathiou, J.A.; Bray, F.; Jemal, A. Recent Global Patterns in Prostate Cancer Incidence and Mortality Rates. *Eur Urol* 2020, *77*, 38–52.
61. Weydert, Z.; Lal-Nag, M.; Mathews-Greiner, L.; Thiel, C.; Cordes, H.; Küpfer, L.; Guye, P.; Kelm, J.M.; Ferrer, M. A 3D Heterotypic Multicellular Tumor Spheroid Assay Platform to Discriminate Drug Effects on Stroma versus Cancer Cells. *SLAS Discovery* **2020**, *25*, 265–276, doi:10.1177/2472555219880194.
62. Courau, T.; Bonnereau, J.; Chicoteau, J.; Bottois, H.; Remark, R.; Assante Miranda, L.; Toubert, A.; Blery, M.; Aparicio, T.; Allez, M.; et al. Cocultures of Human Colorectal Tumor Spheroids with Immune Cells Reveal the Therapeutic Potential of MICA/B and NKG2A Targeting for Cancer Treatment. *J Immunother Cancer* **2019**, *7*, doi:10.1186/s40425-019-0553-9.
63. Drost, J.; Clevers, H. Organoids in Cancer Research. *Nat Rev Cancer* **2018**, *18*, 407–418, doi:10.1038/s41568-018-0007-6.
64. Lancaster, M.A.; Knoblich, J.A. Organogenesis in a Dish: Modeling Development and Disease Using Organoid Technologies. *Science (1979)* **2014**, *345*, doi:10.1126/science.1247125.
65. Quadrato, G.; Brown, J.; Arlotta, P. The Promises and Challenges of Human Brain Organoids as Models of Neuropsychiatric Disease. *Nat Med* **2016**, *22*, 1220–1228, doi:10.1038/nm.4214.
66. Jiang, S.; Zhao, H.; Zhang, W.; Wang, J.; Liu, Y.; Cao, Y.; Zheng, H.; Hu, Z.; Wang, S.; Zhu, Y.; et al. An Automated Organoid Platform with Inter-Organoid Homogeneity and Inter-Patient Heterogeneity. *Cell Rep Med* **2020**, *1*, doi:10.1016/j.xcrm.2020.100161.

67. Maenhoudt, N.; Defraye, C.; Boretto, M.; Jan, Z.; Heremans, R.; Boeckx, B.; Hermans, F.; Arijs, I.; Cox, B.; Van Nieuwenhuysen, E.; et al. Developing Organoids from Ovarian Cancer as Experimental and Preclinical Models. *Stem Cell Reports* **2020**, *14*, 717–729, doi:10.1016/j.stemcr.2020.03.004.
68. Steele, N.G.; Chakrabarti, J.; Wang, J.; Biesiada, J.; Holokai, L.; Chang, J.; Nowacki, L.M.; Hawkins, J.; Mahe, M.; Sundaram, N.; et al. An Organoid-Based Preclinical Model of Human Gastric Cancer. *Cell Mol Gastroenterol Hepatol* **2019**, *7*, 161–184, doi:10.1016/j.jcmgh.2018.09.008.
69. Schmitz, C.H.J.; Rowat, A.C.; Köster, S.; Weitz, D.A. Dropspots: A Picoliter Array in a Microfluidic Device. *Lab Chip* **2009**, *9*, 44–49, doi:10.1039/B809670H.
70. Whitesides, G.M. The Origins and the Future of Microfluidics. *Nature* **2006**, *442*, 368–373, doi:10.1038/nature05058.
71. Ronaldson-Bouchard, K.; Teles, D.; Yeager, K.; Tavakol, D.N.; Zhao, Y.; Chramiec, A.; Tagore, S.; Summers, M.; Stylianos, S.; Tamargo, M.; et al. A Multi-Organ Chip with Matured Tissue Niches Linked by Vascular Flow. *Nat Biomed Eng* **2022**, *6*, 351–371, doi:10.1038/s41551-022-00882-6.
72. Ma, L.-D.; Wang, Y.-T.; Wang, J.-R.; Wu, J.-L.; Meng, X.-S.; Hu, P.; Mu, X.; Liang, Q.-L.; Luo, G.-A. Design and Fabrication of a Liver-on-a-Chip Platform for Convenient, Highly Efficient, and Safe in Situ Perfusion Culture of 3D Hepatic Spheroids. *Lab Chip* **2018**, *18*, 2547–2562, doi:10.1039/C8LC00333E.
73. Leung, C.M.; de Haan, P.; Ronaldson-Bouchard, K.; Kim, G.A.; Ko, J.; Rho, H.S.; Chen, Z.; Habibovic, P.; Jeon, N.L.; Takayama, S.; et al. A Guide to the Organ-on-a-Chip. *Nature Reviews Methods Primers* 2022, *2*.
74. Xu, M.; Shaw, G.; Murphy, M.; Barry, F. Induced Pluripotent Stem Cell-Derived Mesenchymal Stromal Cells Are Functionally and Genetically Different From Bone Marrow-Derived Mesenchymal Stromal Cells. *Stem Cells* **2019**, *37*, 754–765, doi:10.1002/stem.2993.
75. Diederichs, S.; Tuan, R.S. Functional Comparison of Human-Induced Pluripotent Stem Cell-Derived Mesenchymal Cells and Bone Marrow-Derived Mesenchymal Stromal Cells from the Same Donor. *Stem Cells Dev* **2014**, *23*, 1594–1610, doi:10.1089/scd.2013.0477.
76. van den Berg, A.; Mummery, C.L.; Passier, R.; van der Meer, A.D. Personalised Organs-on-Chips: Functional Testing for Precision Medicine. *Lab Chip* **2019**, *19*, 198–205, doi:10.1039/c8lc00827b.
77. Ronaldson-Bouchard, K.; Vunjak-Novakovic, G. Organs-on-a-Chip: A Fast Track for Engineered Human Tissues in Drug Development. *Cell Stem Cell* **2018**, *22*, 310–324, doi:10.1016/j.stem.2018.02.011.
78. Maoz, B.M.; Herland, A.; FitzGerald, E.A.; Grevesse, T.; Vidoudez, C.; Pacheco, A.R.; Sheehy, S.P.; Park, T.-E.; Dauth, S.; Mannix, R.; et al. A Linked Organ-on-Chip Model of the Human Neurovascular Unit Reveals the Metabolic Coupling of Endothelial and Neuronal Cells. *Nat Biotechnol* **2018**, *36*, 865–874, doi:10.1038/nbt.4226.
79. da Ponte, R.M.; Gaio, N.; van Zeijl, H.; Vollebregt, S.; Dijkstra, P.; Dekker, R.; Serdijn, W.A.; Giagka, V. Monolithic Integration of a Smart Temperature Sensor on a Modular Silicon-Based Organ-on-a-Chip Device. *Sens Actuators A Phys* **2021**, *317*, 112439, doi:10.1016/j.sna.2020.112439.
80. Quirós-Solano, W.F.; Gaio, N.; Stassen, O.M.J.A.; Arik, Y.B.; Silvestri, C.; Van Engeland, N.C.A.; Van der Meer, A.; Passier, R.; Sahlgren, C.M.; Bouten, C.V.C.; et al. Microfabricated Tuneable and Transferable Porous PDMS Membranes for Organs-on-Chips. *Sci Rep* **2018**, *8*, 13524, doi:10.1038/s41598-018-31912-6.
81. Campbell, S.B.; Wu, Q.; Yazbeck, J.; Liu, C.; Okhovatian, S.; Radisic, M. Beyond Polydimethylsiloxane: Alternative Materials for Fabrication of Organ-on-a-Chip Devices and Microphysiological Systems. *ACS Biomater Sci Eng* **2021**, *7*, 2880–2899, doi:10.1021/acsbiomaterials.0c00640.
82. Hirama, H.; Satoh, T.; Sugiura, S.; Shin, K.; Onuki-Nagasaki, R.; Kanamori, T.; Inoue, T. Glass-Based Organ-on-a-Chip Device for Restricting Small Molecular Absorption. *J Biosci Bioeng* **2019**, *127*, 641–646, doi:10.1016/j.jbiosc.2018.10.019.
83. Fritschen, A.; Bell, A.K.; Königstein, I.; Stühn, L.; Stark, R.W.; Blaeser, A. Investigation and Comparison of Resin Materials in Transparent DLP-Printing for Application in Cell Culture and Organs-on-a-Chip. *Biomater Sci* **2022**, *10*, 1981–1994, doi:10.1039/D1BM01794B.
84. Warr, C.; Valdoz, J.C.; Bickham, B.P.; Knight, C.J.; Franks, N.A.; Chartrand, N.; Van Ry, P.M.; Christensen, K.A.; Nordin, G.P.; Cook, A.D. Biocompatible PEGDA Resin for 3D Printing. *ACS Appl Bio Mater* **2020**, *3*, 2239–2244, doi:10.1021/acsabm.0c00055.
85. Alsharhan, A.T.; Acevedo, R.; Warren, R.; Sochol, R.D. 3D Microfluidics via Cyclic Olefin Polymer-Based in Situ Direct Laser Writing. *Lab Chip* **2019**, *19*, 2799–2810, doi:10.1039/C9LC00542K.
86. Busek, M.; Nøvik, S.; Aizenshtadt, A.; Amirola-Martinez, M.; Combriat, T.; Grünzner, S.; Krauss, S. Thermoplastic Elastomer (TPE)–Poly(Methyl Methacrylate) (PMMA) Hybrid Devices for Active Pumping PDMS-Free Organ-on-a-Chip Systems. *Biosensors (Basel)* **2021**, *11*, 162, doi:10.3390/bios11050162.
87. Nguyen, T.; Jung, S.H.; Lee, M.S.; Park, T.-E.; Ahn, S.; Kang, J.H. Robust Chemical Bonding of PMMA Microfluidic Devices to Porous PETE Membranes for Reliable Cytotoxicity Testing of Drugs. *Lab Chip* **2019**, *19*, 3706–3713, doi:10.1039/C9LC00338J.
88. Lee, H.-M.; Yu, M.-S.; Kazmi, S.R.; Oh, S.Y.; Rhee, K.-H.; Bae, M.-A.; Lee, B.H.; Shin, D.-S.; Oh, K.-S.; Ceong, H.; et al. Computational Determination of HERG-Related Cardiotoxicity of Drug Candidates. *BMC Bioinformatics* **2019**, *20*, 250, doi:10.1186/s12859-019-2814-5.

89. Chramiec, A.; Teles, D.; Yeager, K.; Marturano-Kruik, A.; Pak, J.; Chen, T.; Hao, L.; Wang, M.; Lock, R.; Tavakol, D.N.; et al. Integrated Human Organ-on-a-Chip Model for Predictive Studies of Anti-Tumor Drug Efficacy and Cardiac Safety. *Lab Chip* **2020**, *20*, 4357–4372, doi:10.1039/D0LC00424C.
90. Liu, Y.; Sakolish, C.; Chen, Z.; Phan, D.T.T.; Bender, R.H.F.; Hughes, C.C.W.; Rusyn, I. Human in Vitro Vascularized Micro-Organ and Micro-Tumor Models Are Reproducible Organ-on-a-Chip Platforms for Studies of Anticancer Drugs. *Toxicology* **2020**, *445*, doi:10.1016/j.tox.2020.152601.
91. Hachey, S.J.; Movsesyan, S.; Nguyen, Q.H.; Burton-Sojo, G.; Tankazyan, A.; Wu, J.; Hoang, T.; Zhao, D.; Wang, S.; Hatch, M.M.; et al. An: In Vitro Vascularized Micro-Tumor Model of Human Colorectal Cancer Recapitulates in Vivo Responses to Standard-of-Care Therapy. *Lab Chip* **2021**, *21*, 1333–1351, doi:10.1039/d0lc01216e.
92. Yu, J.; Lee, S.; Song, J.; Lee, S.R.; Kim, S.; Choi, H.; Kang, H.; Hwang, Y.; Hong, Y.K.; Jeon, N.L. Perfusable Micro-Vascularized 3D Tissue Array for High-Throughput Vascular Phenotypic Screening. *Nano Converg* **2022**, *9*, doi:10.1186/s40580-022-00306-w.
93. Shahrubudin, N.; Lee, T.C.; Ramlan, R. An Overview on 3D Printing Technology: Technological, Materials, and Applications. *Procedia Manuf* **2019**, *35*, 1286–1296, doi:10.1016/j.promfg.2019.06.089.
94. Hwang, S.; Reyes, E.I.; Moon, K.; Rumpf, R.C.; Kim, N.S. Thermo-Mechanical Characterization of Metal/Polymer Composite Filaments and Printing Parameter Study for Fused Deposition Modeling in the 3D Printing Process. *J Electron Mater* **2015**, *44*, 771–777, doi:10.1007/s11664-014-3425-6.
95. Valino, A.D.; Dizon, J.R.C.; Espera, A.H.; Chen, Q.; Messman, J.; Advincula, R.C. Advances in 3D Printing of Thermoplastic Polymer Composites and Nanocomposites. *Prog Polym Sci* **2019**, *98*, 101162, doi:10.1016/j.progpolymsci.2019.101162.
96. Gopinathan, J.; Noh, I. Recent Trends in Bioinks for 3D Printing. *Biomater Res* **2018**, *22*, 11, doi:10.1186/s40824-018-0122-1.
97. Zhu, Y.; Joralmon, D.; Shan, W.; Chen, Y.; Rong, J.; Zhao, H.; Xiao, S.; Li, X. 3D Printing Biomimetic Materials and Structures for Biomedical Applications. *Biodes Manuf* **2021**, *4*, 405–428, doi:10.1007/s42242-020-00117-0.
98. Zhang, B.; Pei, X.; Zhou, C.; Fan, Y.; Jiang, Q.; Ronca, A.; D'Amora, U.; Chen, Y.; Li, H.; Sun, Y.; et al. The Biomimetic Design and 3D Printing of Customized Mechanical Properties Porous Ti6Al4V Scaffold for Load-Bearing Bone Reconstruction. *Mater Des* **2018**, *152*, 30–39, doi:10.1016/j.matdes.2018.04.065.
99. Zennifer, A.; Manivannan, S.; Sethuraman, S.; Kumbar, S.G.; Sundaramurthi, D. 3D Bioprinting and Photocrosslinking: Emerging Strategies & Future Perspectives. *Biomaterials Advances* **2022**, *134*, 112576, doi:10.1016/j.msec.2021.112576.
100. Ouyang, L.; Highley, C.B.; Sun, W.; Burdick, J.A. A Generalizable Strategy for the 3D Bioprinting of Hydrogels from Nonviscous Photo-crosslinkable Inks. *Advanced Materials* **2017**, *29*, 1604983, doi:10.1002/adma.201604983.
101. Wilson, S.A.; Cross, L.M.; Peak, C.W.; Gaharwar, A.K. Shear-Thinning and Thermo-Reversible Nanoengineered Inks for 3D Bioprinting. *ACS Appl Mater Interfaces* **2017**, *9*, 43449–43458, doi:10.1021/acsami.7b13602.
102. Highley, C.B.; Rodell, C.B.; Burdick, J.A. Direct 3D Printing of Shear-Thinning Hydrogels into Self-Healing Hydrogels. *Advanced Materials* **2015**, *27*, 5075–5079, doi:10.1002/adma.201501234.
103. Kuzucu, M.; Vera, G.; Beaumont, M.; Fischer, S.; Wei, P.; Shastri, V.P.; Forget, A. Extrusion-Based 3D Bioprinting of Gradients of Stiffness, Cell Density, and Immobilized Peptide Using Thermogelling Hydrogels. *ACS Biomater Sci Eng* **2021**, *7*, 2192–2197, doi:10.1021/acsbiomaterials.1c00183.
104. Li, W.; Wang, M.; Ma, H.; Chapa-Villarreal, F.A.; Lobo, A.O.; Zhang, Y.S. Stereolithography Apparatus and Digital Light Processing-Based 3D Bioprinting for Tissue Fabrication. *iScience* **2023**, *26*, 106039, doi:10.1016/j.isci.2023.106039.
105. Yu, C.; Ma, X.; Zhu, W.; Wang, P.; Miller, K.L.; Stupin, J.; Koroleva-Maharajh, A.; Hairabedian, A.; Chen, S. Scanningless and Continuous 3D Bioprinting of Human Tissues with Decellularized Extracellular Matrix. *Biomaterials* **2019**, *194*, 1–13, doi:10.1016/j.biomaterials.2018.12.009.
106. Godar, D.E.; Gurunathan, C.; Ilev, I. 3D Bioprinting with UVA1 Radiation and Photoinitiator Irgacure 2959: Can the ASTM Standard L929 Cells Predict Human Stem Cell Cytotoxicity? *Photochem Photobiol* **2019**, *95*, 581–586, doi:10.1111/php.13028.
107. Gittard, S.D. Two-Photon Polymerization Microstructuring in Regenerative Medicine. *Frontiers in Bioscience* **2013**, *E5*, E642, doi:10.2741/E642.
108. Tromayer, M.; Gruber, P.; Markovic, M.; Rosspeintner, A.; Vauthey, E.; Redl, H.; Ovsianikov, A.; Liska, R. A Biocompatible Macromolecular Two-Photon Initiator Based on Hyaluronan. *Polym Chem* **2017**, *8*, 451–460, doi:10.1039/c6py01787h.
109. Li, Z.; Torgersen, J.; Ajami, A.; Mühleder, S.; Qin, X.; Husinsky, W.; Holnthoner, W.; Ovsianikov, A.; Stampfl, J.; Liska, R. Initiation Efficiency and Cytotoxicity of Novel Water-Soluble Two-Photon Photoinitiators for Direct 3D Microfabrication of Hydrogels. *RSC Adv* **2013**, *3*, 15939–15946, doi:10.1039/c3ra42918k.

110. Masuma, R.; Kashima, S.; Kurasaki, M.; Okuno, T. Effects of UV Wavelength on Cell Damages Caused by UV Irradiation in PC12 Cells. *J Photochem Photobiol B* **2013**, *125*, 202–208, doi:10.1016/j.jphotobiol.2013.06.003.
111. Moon, S.H.; Choi, H.N.; Yang, Y.J. Natural/Synthetic Polymer Materials for Bioink Development. *Biotechnology and Bioprocess Engineering* **2022**, *27*, 482–493, doi:10.1007/s12257-021-0418-1.
112. Muthusamy, S.; Kannan, S.; Lee, M.; Sanjairaj, V.; Lu, W.F.; Fuh, J.Y.H.; Sriram, G.; Cao, T. 3D Bioprinting and Microscale Organization of Vascularized Tissue Constructs Using Collagen-based Bioink. *Biotechnol Bioeng* **2021**, *118*, 3150–3163, doi:10.1002/bit.27838.
113. Shoulders, M.D.; Raines, R.T. Collagen Structure and Stability. *Annu Rev Biochem* **2009**, *78*, 929–958, doi:10.1146/annurev.biochem.77.032207.120833.
114. Kadler, K.E.; Baldock, C.; Bella, J.; Boot-Handford, R.P. Collagens at a Glance. *J Cell Sci* **2007**, *120*, 1955–1958, doi:10.1242/jcs.03453.
115. Sun, M.; Sun, X.; Wang, Z.; Guo, S.; Yu, G.; Yang, H. Synthesis and Properties of Gelatin Methacryloyl (GelMA) Hydrogels and Their Recent Applications in Load-Bearing Tissue. *Polymers (Basel)* **2018**, *10*, 1290, doi:10.3390/polym10111290.
116. Wang, X.; Ao, Q.; Tian, X.; Fan, J.; Tong, H.; Hou, W.; Bai, S. Gelatin-Based Hydrogels for Organ 3D Bioprinting. *Polymers (Basel)* **2017**, *9*, 401, doi:10.3390/polym9090401.
117. Foox, M.; Zilberman, M. Drug Delivery from Gelatin-Based Systems. *Expert Opin Drug Deliv* **2015**, *12*, 1547–1563, doi:10.1517/17425247.2015.1037272.
118. Lee, B.H.; Shirahama, H.; Cho, N.-J.; Tan, L.P. Efficient and Controllable Synthesis of Highly Substituted Gelatin Methacrylamide for Mechanically Stiff Hydrogels. *RSC Adv* **2015**, *5*, 106094–106097, doi:10.1039/C5RA22028A.
119. Sharifi, S.; Sharifi, H.; Akbari, A.; Chodosh, J. Systematic Optimization of Visible Light-Induced Crosslinking Conditions of Gelatin Methacryloyl (GelMA). *Sci Rep* **2021**, *11*, 23276, doi:10.1038/s41598-021-02830-x.
120. Zhu, M.; Wang, Y.; Ferracci, G.; Zheng, J.; Cho, N.-J.; Lee, B.H. Gelatin Methacryloyl and Its Hydrogels with an Exceptional Degree of Controllability and Batch-to-Batch Consistency. *Sci Rep* **2019**, *9*, 6863, doi:10.1038/s41598-019-42186-x.
121. Kneser, U.; Voogd, A.; Ohnolz, J.; Buettner, O.; Stangenberg, L.; Zhang, Y.H.; Stark, G.B.; Schaefer, D.J. Fibrin Gel-Immobilized Primary Osteoblasts in Calcium Phosphate Bone Cement: In Vivo Evaluation with Regard to Application as Injectable Biological Bone Substitute. *Cells Tissues Organs* **2005**, *179*, 158–169, doi:10.1159/000085951.
122. Abelseth, E.; Abelseth, L.; De la Vega, L.; Beyer, S.T.; Wadsworth, S.J.; Willerth, S.M. 3D Printing of Neural Tissues Derived from Human Induced Pluripotent Stem Cells Using a Fibrin-Based Bioink. *ACS Biomater Sci Eng* **2019**, *5*, 234–243, doi:10.1021/acsbiomaterials.8b01235.
123. Piard, C.; Baker, H.; Kamalitdinov, T.; Fisher, J. Bioprinted Osteon-like Scaffolds Enhance in Vivo Neovascularization. *Biofabrication* **2019**, *11*, 025013, doi:10.1088/1758-5090/ab078a.
124. Ding, Y.-W.; Zhang, X.-W.; Mi, C.-H.; Qi, X.-Y.; Zhou, J.; Wei, D.-X. Recent Advances in Hyaluronic Acid-Based Hydrogels for 3D Bioprinting in Tissue Engineering Applications. *Smart Mater Med* **2023**, *4*, 59–68, doi:10.1016/j.smaim.2022.07.003.
125. Collins, M.N.; Birkinshaw, C. Hyaluronic Acid Based Scaffolds for Tissue Engineering—A Review. *Carbohydr Polym* **2013**, *92*, 1262–1279, doi:10.1016/j.carbpol.2012.10.028.
126. Perng, C.-K.; Wang, Y.-J.; Tsi, C.-H.; Ma, H. In Vivo Angiogenesis Effect of Porous Collagen Scaffold with Hyaluronic Acid Oligosaccharides. *Journal of Surgical Research* **2011**, *168*, 9–15, doi:10.1016/j.jss.2009.09.052.
127. Wang, X.; He, J.; Wang, Y.; Cui, F.-Z. Hyaluronic Acid-Based Scaffold for Central Neural Tissue Engineering. *Interface Focus* **2012**, *2*, 278–291, doi:10.1098/rsfs.2012.0016.
128. Mazzocchi, A.; Devarasetty, M.; Huntwork, R.; Soker, S.; Skardal, A. Optimization of Collagen Type I-Hyaluronan Hybrid Bioink for 3D Bioprinted Liver Microenvironments. *Biofabrication* **2018**, *11*, 015003, doi:10.1088/1758-5090/aae543.
129. Khunmanee, S.; Jeong, Y.; Park, H. Crosslinking Method of Hyaluronic-Based Hydrogel for Biomedical Applications. *J Tissue Eng* **2017**, *8*, 204173141772646, doi:10.1177/2041731417726464.
130. Wu, Q.; Therriault, D.; Heuzey, M.-C. Processing and Properties of Chitosan Inks for 3D Printing of Hydrogel Microstructures. *ACS Biomater Sci Eng* **2018**, *4*, 2643–2652, doi:10.1021/acsbiomaterials.8b00415.
131. Taghizadeh, M.; Taghizadeh, A.; Yazdi, M.K.; Zarrintaj, P.; Stadler, F.J.; Ramsey, J.D.; Habibzadeh, S.; Hosseini Rad, S.; Naderi, G.; Saeb, M.R.; et al. Chitosan-Based Inks for 3D Printing and Bioprinting. *Green Chemistry* **2022**, *24*, 62–101, doi:10.1039/D1GC01799C.
132. He, Y.; Derakhshanfar, S.; Zhong, W.; Li, B.; Lu, F.; Xing, M.; Li, X. Characterization and Application of Carboxymethyl Chitosan-Based Bioink in Cartilage Tissue Engineering. *J Nanomater* **2020**, *2020*, 1–11, doi:10.1155/2020/2057097.
133. Ahmad Raus, R.; Wan Nawawi, W.M.F.; Nasaruddin, R.R. Alginate and Alginate Composites for Biomedical Applications. *Asian J Pharm Sci* **2021**, *16*, 280–306, doi:10.1016/j.ajps.2020.10.001.

134. Emami, Z.; Ehsani, M.; Zandi, M.; Foudazi, R. Controlling Alginate Oxidation Conditions for Making Alginate-Gelatin Hydrogels. *Carbohydr Polym* **2018**, *198*, 509–517, doi:10.1016/j.carbpol.2018.06.080.
135. Zhang, X.; Wang, K.; Hu, J.; Zhang, Y.; Dai, Y.; Xia, F. Role of a High Calcium Ion Content in Extending the Properties of Alginate Dual-Crosslinked Hydrogels. *J Mater Chem A Mater* **2020**, *8*, 25390–25401, doi:10.1039/D0TA09315G.
136. Lee, K.Y.; Mooney, D.J. Alginate: Properties and Biomedical Applications. *Prog Polym Sci* **2012**, *37*, 106–126, doi:10.1016/j.progpolymsci.2011.06.003.
137. Keane, T.J.; Swinehart, I.T.; Badylak, S.F. Methods of Tissue Decellularization Used for Preparation of Biologic Scaffolds and in Vivo Relevance. *Methods* **2015**, *84*, 25–34, doi:10.1016/j.ymeth.2015.03.005.
138. Hussey, G.S.; Dziki, J.L.; Badylak, S.F. Extracellular Matrix-Based Materials for Regenerative Medicine. *Nat Rev Mater* **2018**, *3*, 159–173, doi:10.1038/s41578-018-0023-x.
139. Kim, B.S.; Das, S.; Jang, J.; Cho, D.-W. Decellularized Extracellular Matrix-Based Bioinks for Engineering Tissue- and Organ-Specific Microenvironments. *Chem Rev* **2020**, *120*, 10608–10661, doi:10.1021/acs.chemrev.9b00808.
140. Ma, B.; Wang, X.; Wu, C.; Chang, J. Crosslinking Strategies for Preparation of Extracellular Matrix-Derived Cardiovascular Scaffolds. *Regen Biomater* **2014**, *1*, 81–89, doi:10.1093/rb/rbu009.
141. Capuana, E.; Lopresti, F.; Ceraulo, M.; La Carrubba, V. Poly-l-Lactic Acid (PLLA)-Based Biomaterials for Regenerative Medicine: A Review on Processing and Applications. *Polymers (Basel)* **2022**, *14*, 1153, doi:10.3390/polym14061153.
142. Donate, R.; Monzón, M.; Alemán-Domínguez, M.E. Additive Manufacturing of PLA-Based Scaffolds Intended for Bone Regeneration and Strategies to Improve Their Biological Properties. *e-Polymers* **2020**, *20*, 571–599, doi:10.1515/epoly-2020-0046.
143. Muthe, L.P.; Pickering, K.; Gauss, C. A Review of 3D/4D Printing of Poly-Lactic Acid Composites with Bio-Derived Reinforcements. *Composites Part C: Open Access* **2022**, *8*, 100271, doi:10.1016/j.jcomc.2022.100271.
144. Tan, Y.J.; Tan, X.; Yeong, W.Y.; Tor, S.B. Hybrid Microscaffold-Based 3D Bioprinting of Multi-Cellular Constructs with High Compressive Strength: A New Biofabrication Strategy. *Sci Rep* **2016**, *6*, 39140, doi:10.1038/srep39140.
145. Choe, G.; Lee, M.; Oh, S.; Seok, J.M.; Kim, J.; Im, S.; Park, S.A.; Lee, J.Y. Three-Dimensional Bioprinting of Mesenchymal Stem Cells Using an Osteoinductive Bioink Containing Alginate and BMP-2-Loaded PLGA Nanoparticles for Bone Tissue Engineering. *Biomaterials Advances* **2022**, *136*, 212789, doi:10.1016/j.bioadv.2022.212789.
146. Gao, G.; Lee, J.H.; Jang, J.; Lee, D.H.; Kong, J.-S.; Kim, B.S.; Choi, Y.-J.; Jang, W.B.; Hong, Y.J.; Kwon, S.-M.; et al. Tissue Engineered Bio-Blood-Vessels Constructed Using a Tissue-Specific Bioink and 3D Coaxial Cell Printing Technique: A Novel Therapy for Ischemic Disease. *Adv Funct Mater* **2017**, *27*, 1700798, doi:10.1002/adfm.201700798.
147. Naseri, E.; Butler, H.; MacNevin, W.; Ahmed, M.; Ahmadi, A. Low-Temperature Solvent-Based 3D Printing of PLGA: A Parametric Printability Study. *Drug Dev Ind Pharm* **2020**, *46*, 173–178, doi:10.1080/03639045.2019.1711389.
148. Arcaute, K.; Mann, B.; Wicker, R. Stereolithography of Spatially Controlled Multi-Material Bioactive Poly(Ethylene Glycol) Scaffolds. *Acta Biomater* **2010**, *6*, 1047–1054, doi:10.1016/j.actbio.2009.08.017.
149. Tu, X.; Wang, L.; Wei, J.; Wang, B.; Tang, Y.; Shi, J.; Zhang, Z.; Chen, Y. 3D Printed PEGDA Microstructures for Gelatin Scaffold Integration and Neuron Differentiation. *Microelectron Eng* **2016**, *158*, 30–34, doi:10.1016/j.mee.2016.03.007.
150. Bandyopadhyay, A.; Mandal, B.B.; Bhardwaj, N. 3D Bioprinting of Photo-crosslinkable Silk Methacrylate (SilMA)-polyethylene Glycol Diacrylate (PEGDA) Bioink for Cartilage Tissue Engineering. *J Biomed Mater Res A* **2022**, *110*, 884–898, doi:10.1002/jbm.a.37336.
151. Fathi, A.; Kermani, F.; Behnamghader, A.; Banijamali, S.; Mozafari, M.; Baino, F.; Kargozar, S. Three-Dimensionally Printed Polycaprolactone/Multicomponent Bioactive Glass Scaffolds for Potential Application in Bone Tissue Engineering. *Biomedical Glasses* **2020**, *6*, 57–69, doi:10.1515/bglass-2020-0006.
152. Elomaa, L.; Kokkari, A.; Närhi, T.; Seppälä, J. V. Porous 3D Modeled Scaffolds of Bioactive Glass and Photocrosslinkable Poly(ε-Caprolactone) by Stereolithography. *Compos Sci Technol* **2013**, *74*, 99–106, doi:10.1016/j.compscitech.2012.10.014.
153. Yang, X.; Wang, Y.; Zhou, Y.; Chen, J.; Wan, Q. The Application of Polycaprolactone in Three-Dimensional Printing Scaffolds for Bone Tissue Engineering. *Polymers (Basel)* **2021**, *13*, 2754, doi:10.3390/polym13162754.
154. Cai, Z.; Wan, Y.; Becker, M.L.; Long, Y.-Z.; Dean, D. Poly(Propylene Fumarate)-Based Materials: Synthesis, Functionalization, Properties, Device Fabrication and Biomedical Applications. *Biomaterials* **2019**, *208*, 45–71, doi:10.1016/j.biomaterials.2019.03.038.
155. Walker, J.M.; Bodamer, E.; Krebs, O.; Luo, Y.; Kleinfehn, A.; Becker, M.L.; Dean, D. Effect of Chemical and Physical Properties on the In Vitro Degradation of 3D Printed High Resolution Poly(Propylene Fumarate) Scaffolds. *Biomacromolecules* **2017**, *18*, 1419–1425, doi:10.1021/acs.biomac.7b00146.

156. Wang, S.; Lu, L.; Yaszemski, M.J. Bone-Tissue-Engineering Material Poly(Propylene Fumarate): Correlation between Molecular Weight, Chain Dimensions, and Physical Properties. *Biomacromolecules* **2006**, *7*, 1976–1982, doi:10.1021/bm060096a.
157. Bordonaro, M.; Lazarova, D.L.; Augenlicht, L.H.; Sartorelli, A.C. Estimates of the World-Wide Prevalence of Cancer for 25 Sites in the Adult Population. *Int J Cancer* **2002**, *97*, 72–81, doi:10.1002/ijc.1571.
158. Sztankovics, D.; Moldvai, D.; Petővári, G.; Gelencsér, R.; Krencz, I.; Raffay, R.; Dankó, T.; Sebestyén, A. 3D Bioprinting and the Revolution in Experimental Cancer Model Systems—A Review of Developing New Models and Experiences with in Vitro 3D Bioprinted Breast Cancer Tissue-Mimetic Structures. *Pathology and Oncology Research* **2023**, *29*, doi:10.3389/pore.2023.1610996.
159. Zhou, X.; Zhu, W.; Nowicki, M.; Miao, S.; Cui, H.; Holmes, B.; Glazer, R.I.; Zhang, L.G. 3D Bioprinting a Cell-Laden Bone Matrix for Breast Cancer Metastasis Study. *ACS Appl Mater Interfaces* **2016**, *8*, 30017–30026, doi:10.1021/acsami.6b10673.
160. Xu, K.; Huang, Y.; Wu, M.; Yin, J.; Wei, P. 3D Bioprinting of Multi-Cellular Tumor Microenvironment for Prostate Cancer Metastasis. *Biofabrication* **2023**, *15*, 035020, doi:10.1088/1758-5090/acd960.
161. Pulido, C.; Vendrell, I.; Ferreira, A.R.; Casimiro, S.; Mansinho, A.; Alho, I.; Costa, L. Bone Metastasis Risk Factors in Breast Cancer. *Ecancermedicalscience* 2017, *11*.
162. Huang, T.Q.; Qu, X.; Liu, J.; Chen, S. 3D Printing of Biomimetic Microstructures for Cancer Cell Migration. *Biomed Microdevices* **2014**, *16*, 127–132, doi:10.1007/s10544-013-9812-6.
163. Ning, L.; Shim, J.; Tomov, M.L.; Liu, R.; Mehta, R.; Mingee, A.; Hwang, B.; Jin, L.; Mantalaris, A.; Xu, C.; et al. A 3D Bioprinted in Vitro Model of Neuroblastoma Recapitulates Dynamic Tumor-Endothelial Cell Interactions Contributing to Solid Tumor Aggressive Behavior. *Advanced Science* **2022**, *9*, doi:10.1002/advs.202200244